High Resolution TEM

- K. Ishizuka (1980) ***"Contrast Transfer of Crystal Images in TEM"***, Ultramicroscopy **5**,pages 55-65.
- L. Reimer (1993) ***"Transmission Electron Microscopy"***, Springer Verlag, Berlin.
- J.C.H. Spence (1988), ***"Experimental High Resolution Electron Microscopy"***, Oxford University Press, New York.

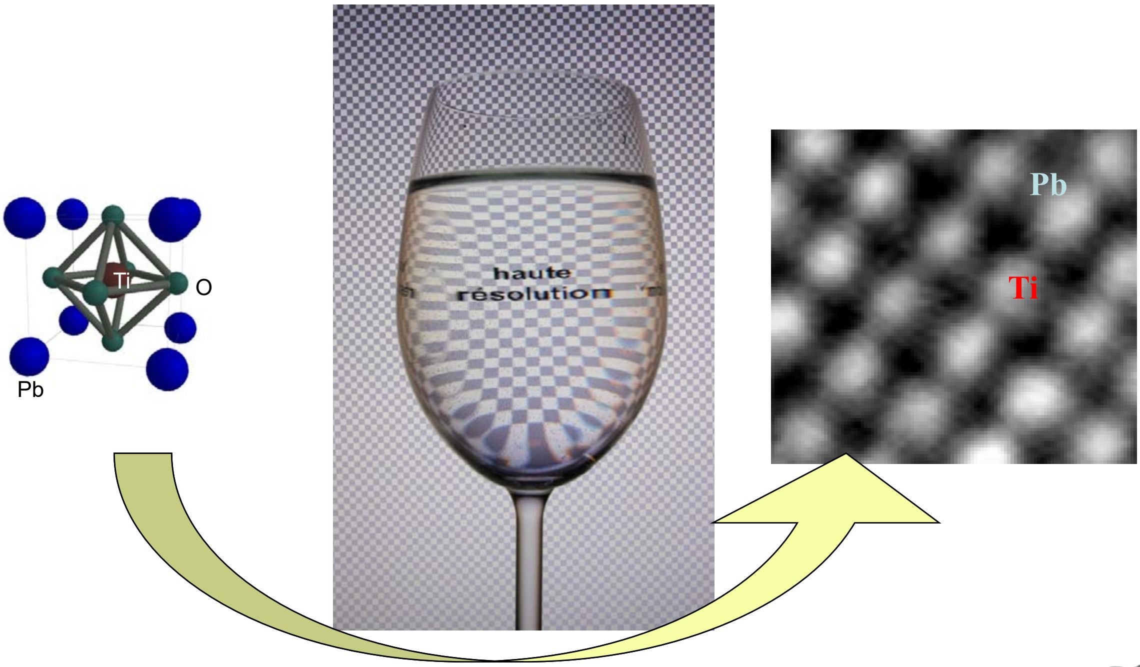

High resolution….?!

electron at 300keV:

- v = 2.33 10^{-8} m/s (0.78 c)
- λ = 0.00197nm
- θ_{diff} = 10^{-3} rad

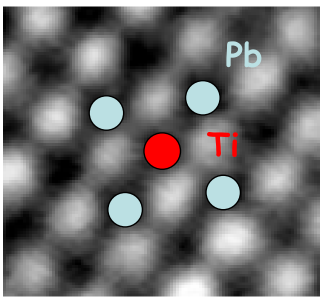

Atomic resolution…?

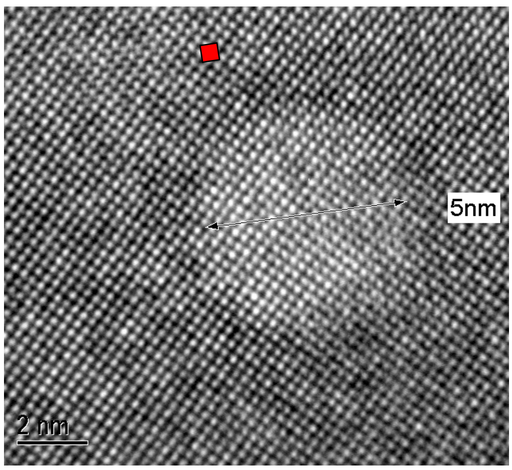

Precipitate in a ceramic: $PbTiO_3$

the TEM in “high-resolution” mode

A high-resolution image is an interference image of the transmitted and the diffracted beams!

Diffracted electrons: coherent elastic scattering (the electrons have seen the crystal lattice)

The quality of the image depends on the optical system that makes the beams interfere

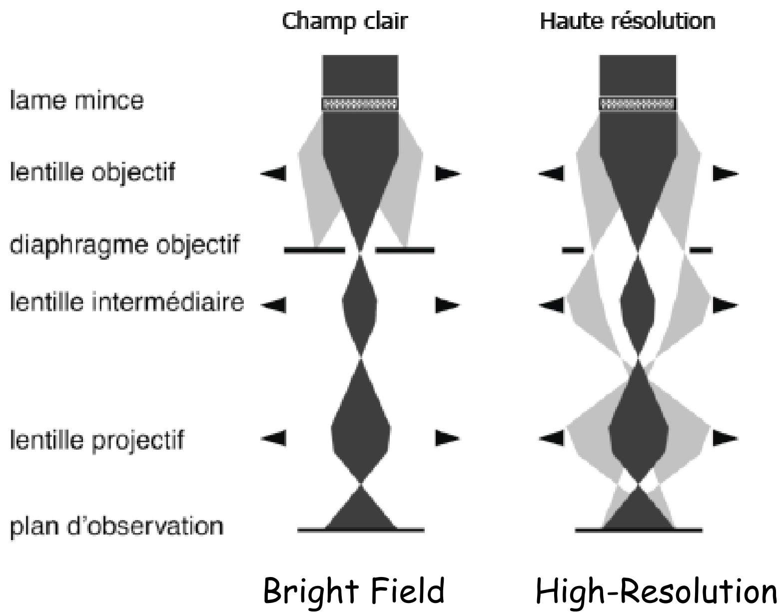

Bright Field Imaging

Diffraction Contrast, Au (nano-) particles on C film

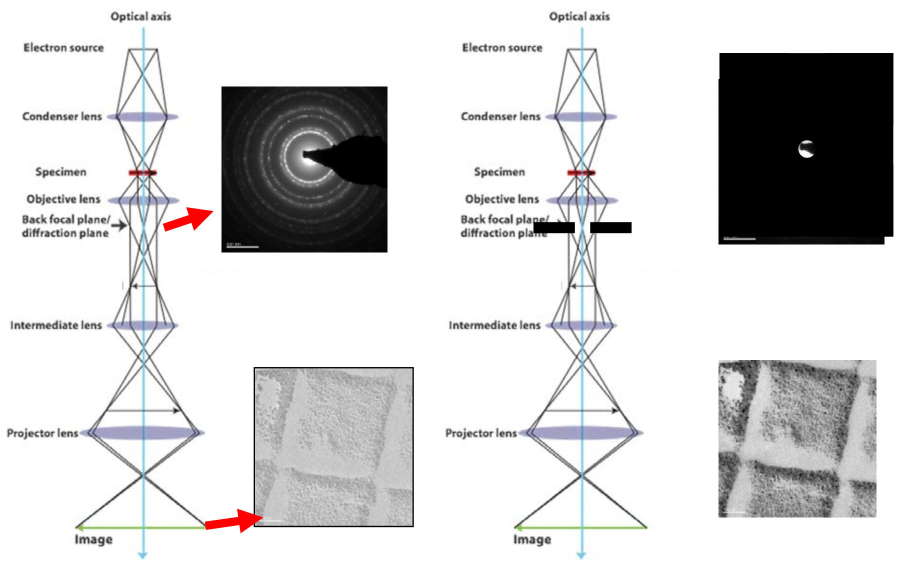

High-resolution image and its FFT

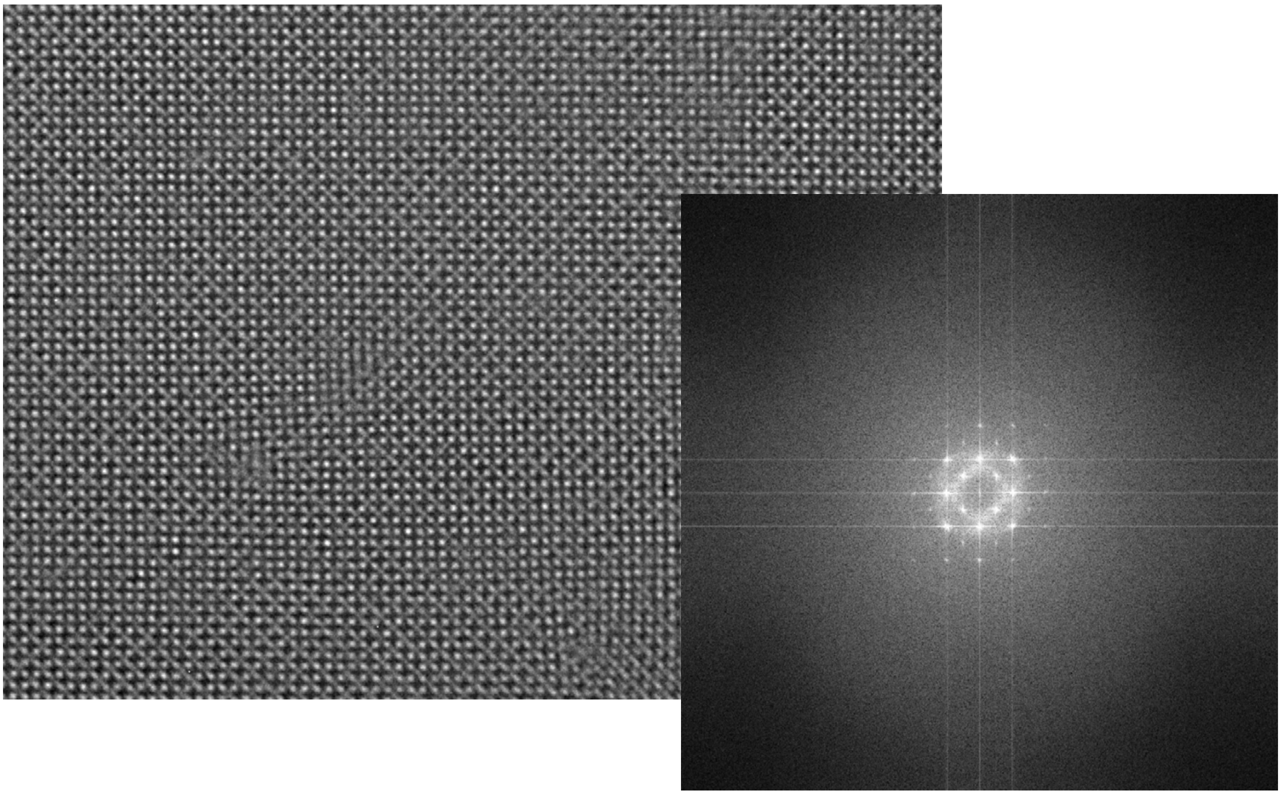

FFT filtering

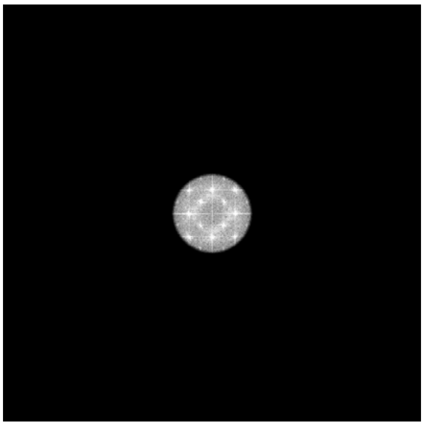

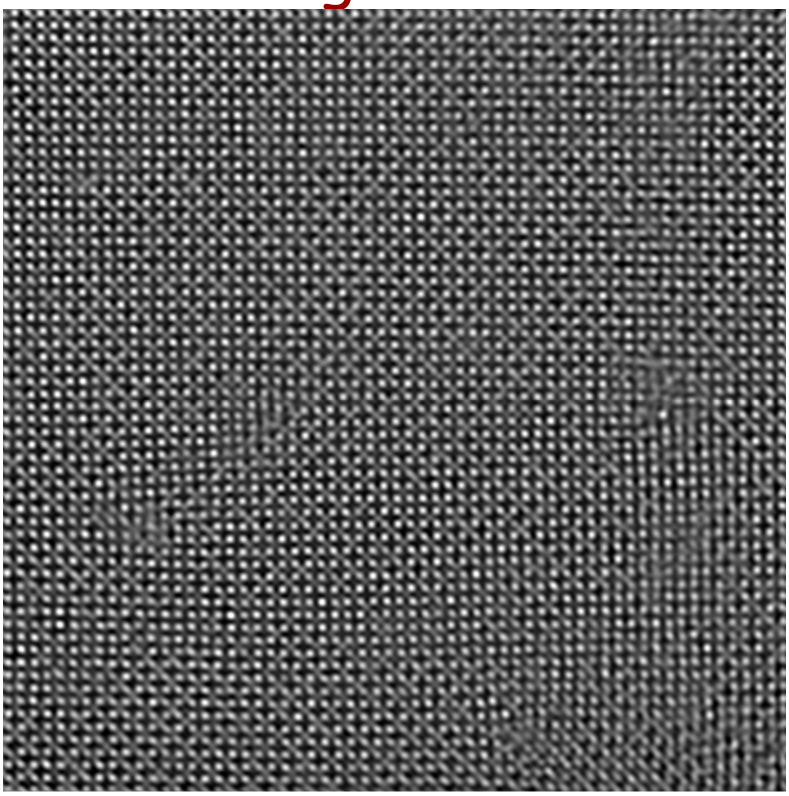

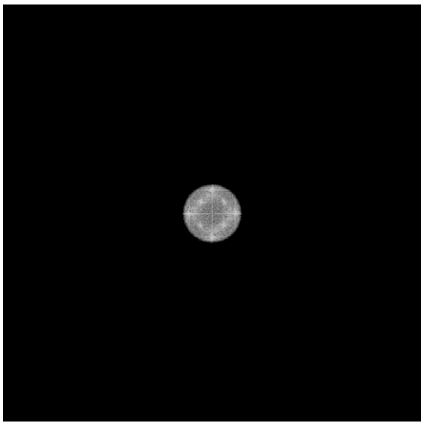

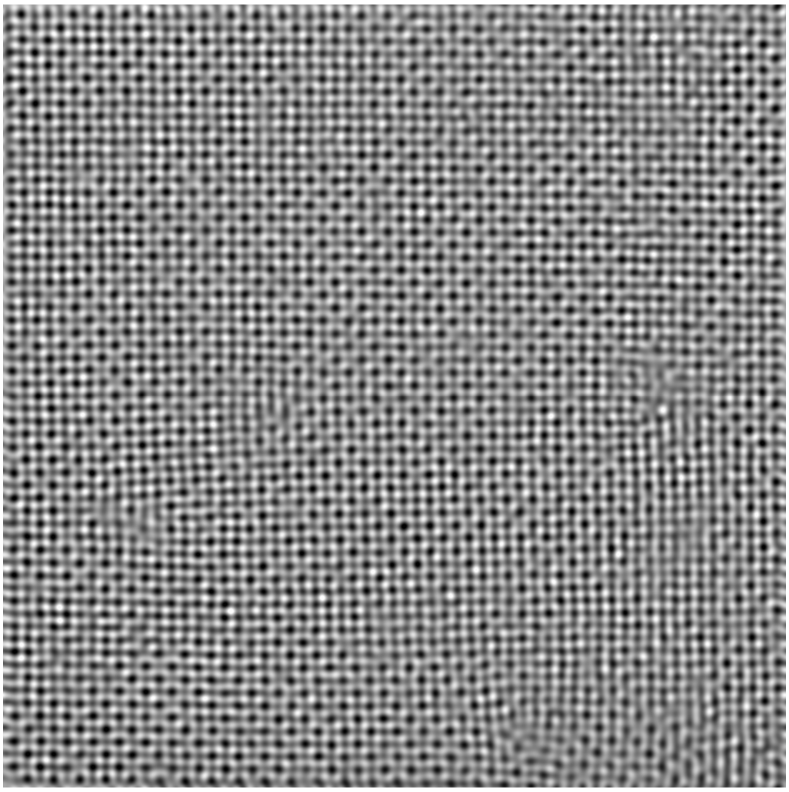

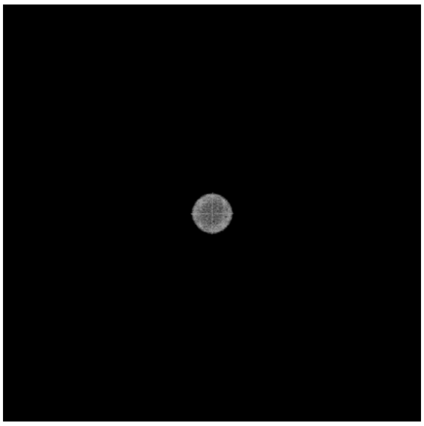

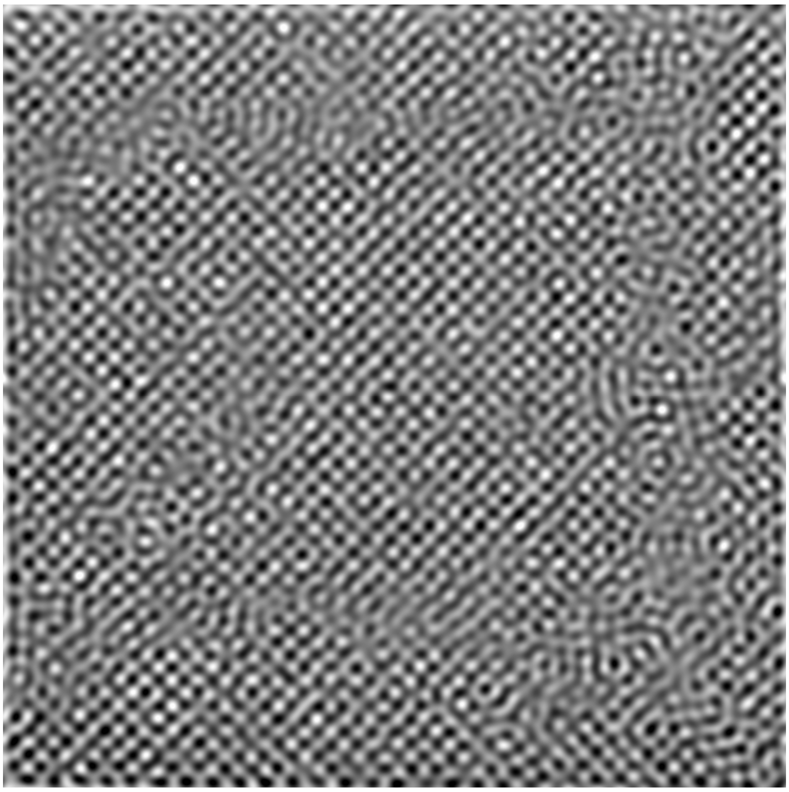

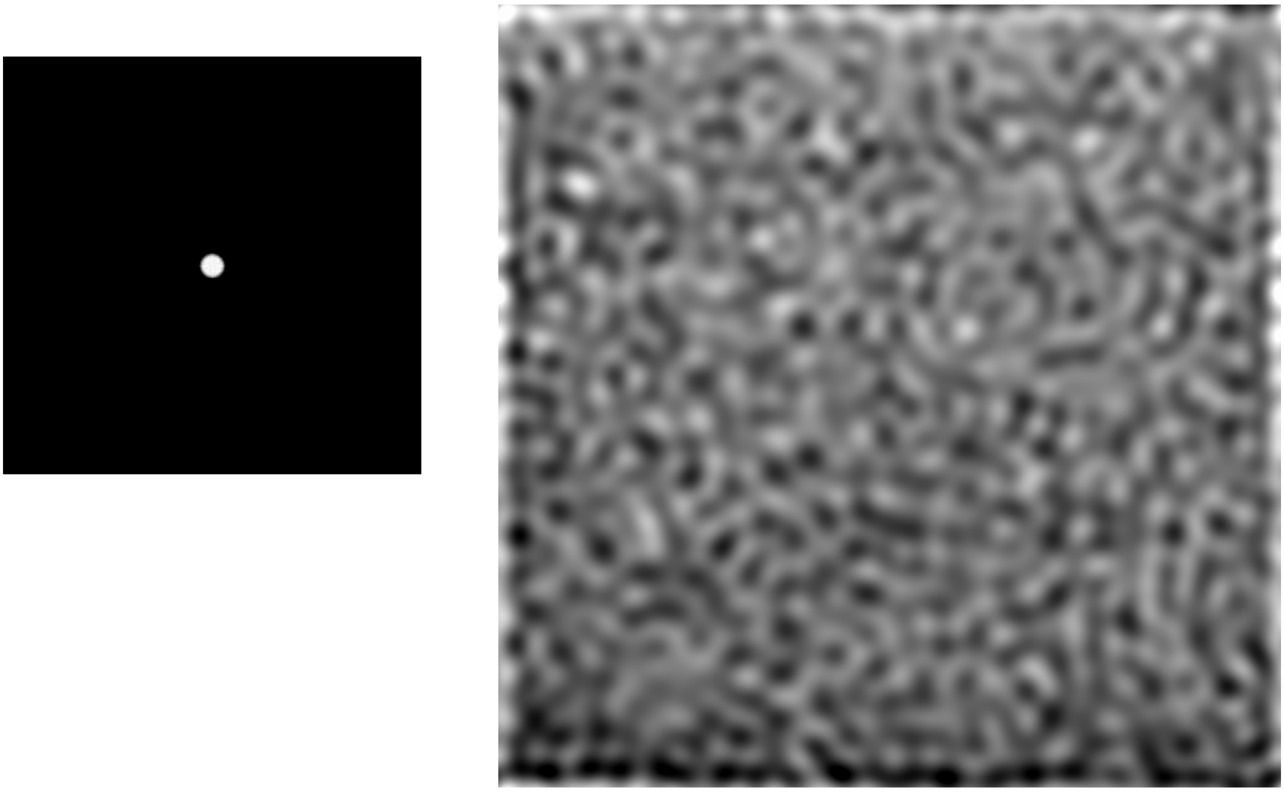

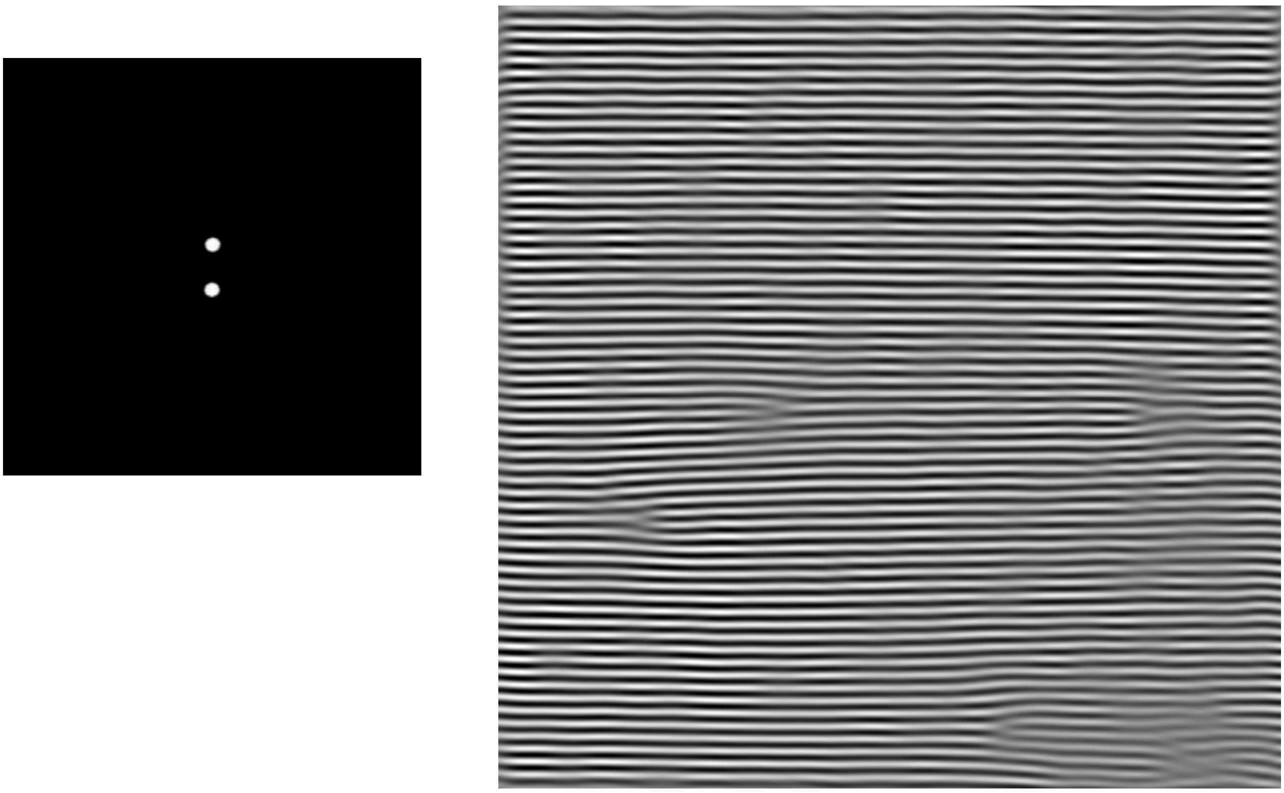

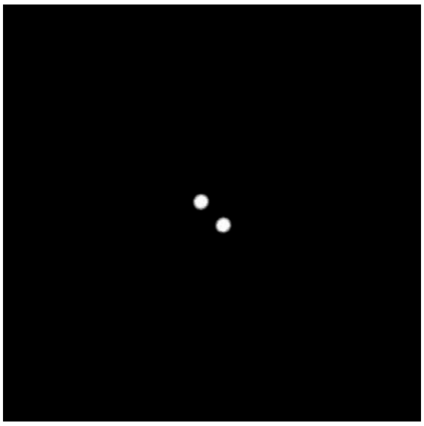

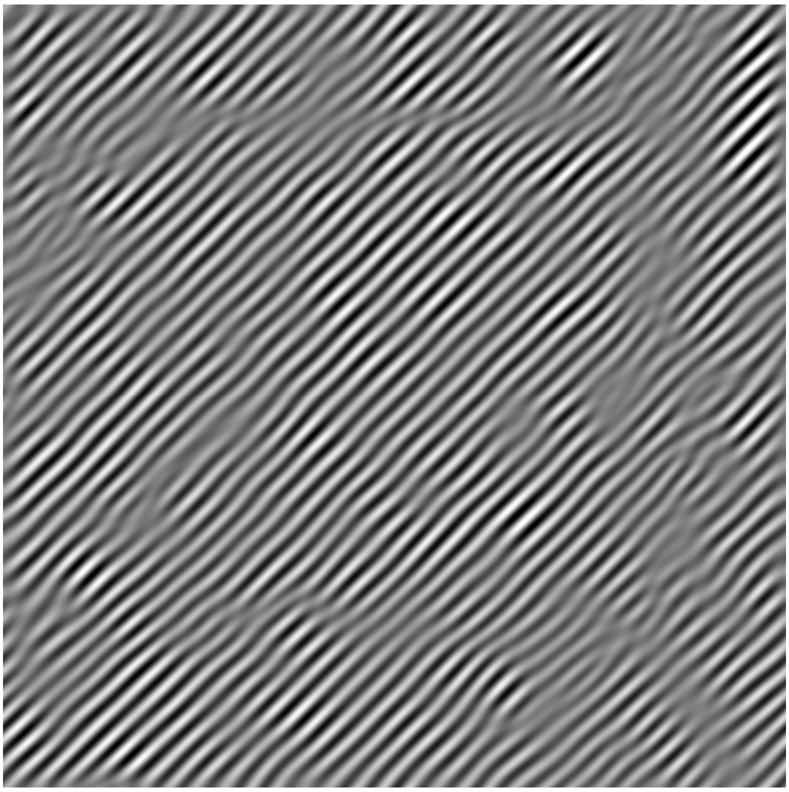

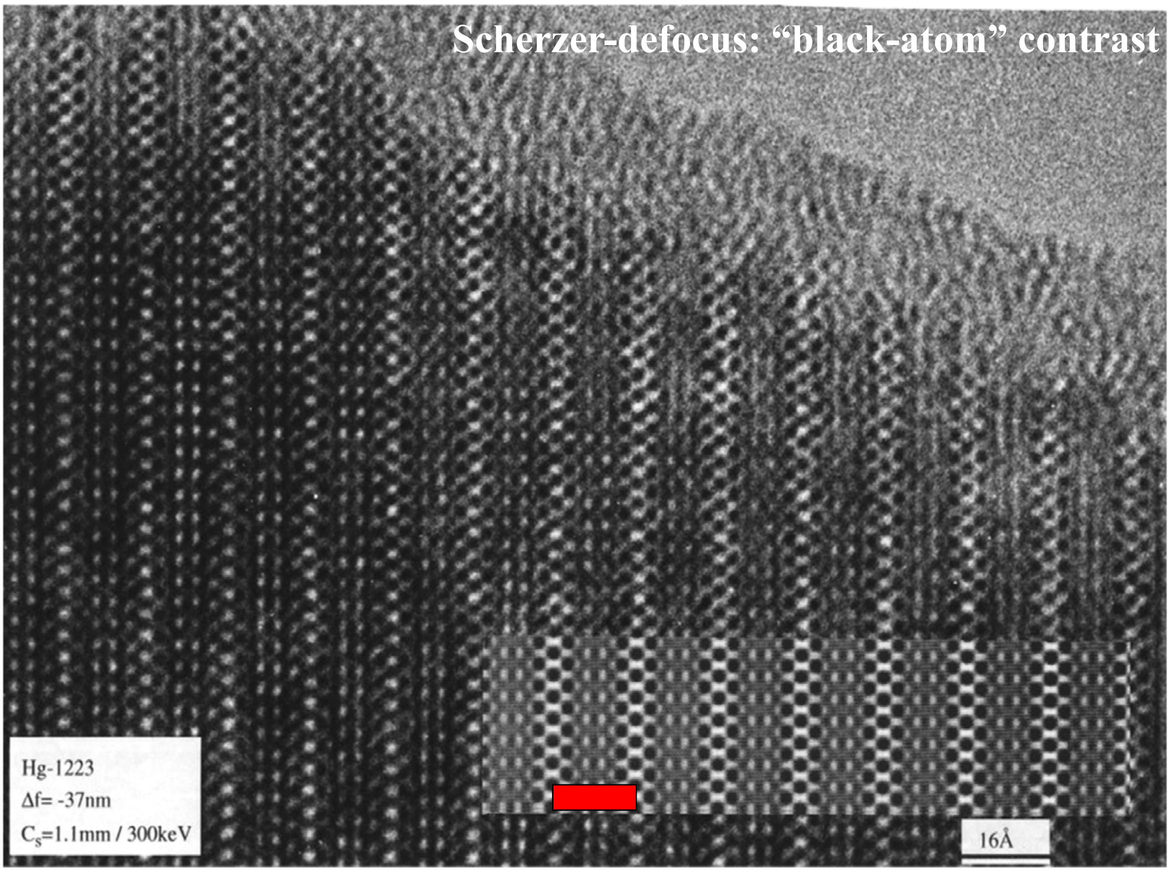
Scherzer-defocus: “black-atom” contrast
Hg-1223
Δf= -37nm
Cs=1.1mm / 300keV
16Å

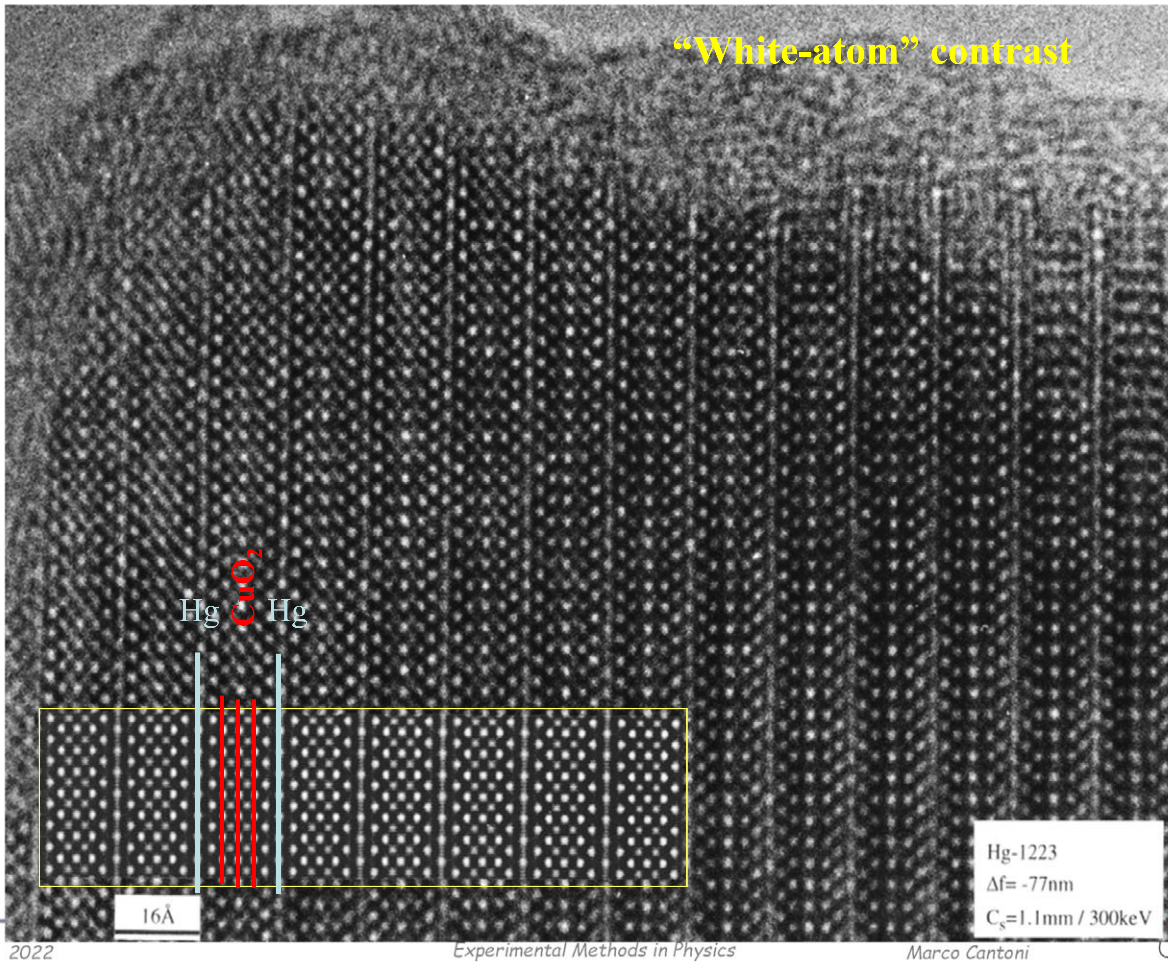

High-resolution

- The image should resemble the atomic structure !
- Atoms…?
  Thin samples: atom columns: orientation of the sample (incident beam // atom columns)
- The observed contrast varies with thickness and defocalisation…!
- Need to compare with simulations !

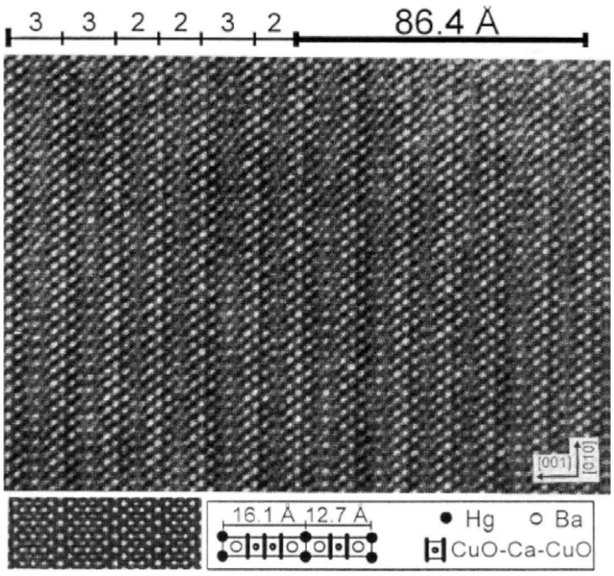

The objective lens

- Field with rotational symmetry
- Lorenz Force : **F** = -e **v** ^ **B**
  e on optical axis: **F** = 0
  e not on optical axis : deviated
  optical axis: symmetry axis

- Scherzer 1936:
- Magnetic lens with rotational symmetry:
  Aberration coefficients:
  C_s: spherical
  C_c: chromatical
  - Always positive !!

$$C_s = \frac{1}{16}\int_{z_o}^{z_i}\left\{b^4h^4 + 2\left(hb' + h'b\right)^2 h^2 + 2b^2h^2h'^2\right\}dz$$

$$C_c = \frac{1}{4}\int_{z_o}^{z_i} b^2h^2 dz$$

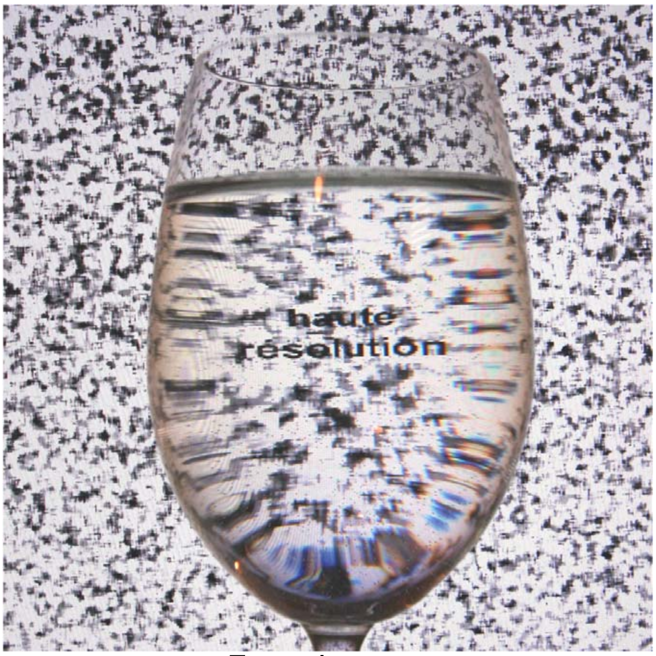

Example:
λ= 0.00197nm, C_s = 1 mm
D_{res} = 1.8 10^{-10} = 1.8Å

Resolution limit: $D_{res} = 0.66\lambda^{3/4}C_s^{1/4}$

Image formation

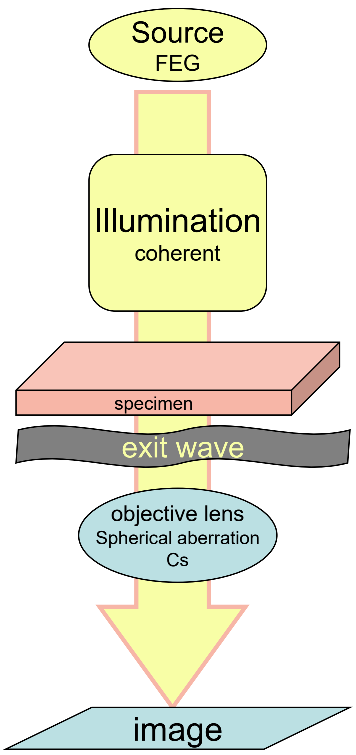

- Illumination

$$\Psi(\vec{\mathbf{r}}) = \Psi_0 \exp^{2\pi i \vec{\mathbf{k}}\cdot\vec{\mathbf{r}}}$$

- Sample

$$\Psi_o(\vec{\mathbf{x}}) = exp\left[-i\sigma V_p(\vec{\mathbf{x}};z)\right] \cong 1 - i\sigma V_p(\vec{\mathbf{x}};z)$$

- objective lens

$$T(\vec{\mathbf{h}}) = \exp\left[2\pi i\chi(\vec{\mathbf{h}})\right] \quad avec \quad \chi(\vec{\mathbf{h}}) = 0.25C_s\lambda^3h^4 + 0.5\Delta z\lambda h^2$$

$$\Psi_i(\vec{\mathbf{x}}) = \Psi_o(\vec{\mathbf{x}}) \otimes T(\vec{\mathbf{x}})$$

- Image, contrast

$$\mathrm{I_i}(\vec{\mathbf{x}}) = \Psi_i(\vec{\mathbf{x}})\Psi_i^*(\vec{\mathbf{x}})$$

sample = phase objet

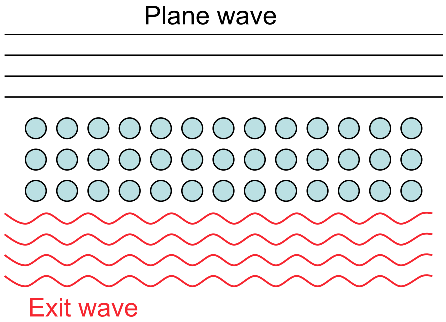

Cristal potential

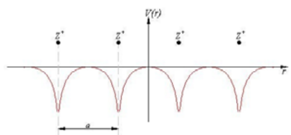

Cristal potential = phase object

Wave vector in vacuum:

$$k = \sqrt{2me(E) / h^2}$$

Wave vector in a potential:

$$k = \sqrt{2me(E + V(\vec{r})) / h^2}$$

Phase shift $\Delta\alpha$ due to the cristal potential V_p:

$$\Delta\alpha = \frac{\sigma}{2\pi} V_p(\vec{x}, z)$$

$$\sigma = \pi / \lambda E$$

Exit wave function: $\Psi_o(\mathbf{\vec{x}}) = exp\left[-i\sigma V_p(\mathbf{\vec{x}}; z)\right]$

WPOA

- Weak phase object approximation:

$$\Psi_o(\mathbf{\vec{x}}) = exp\left[-i\sigma V_p(\mathbf{\vec{x}}; z)\right] \cong 1 - i\sigma V_p(\mathbf{\vec{x}}; z)$$

No absorbtion,effect of the object on the outgoing wave: only phase shift

The exit wave function contains the information about the structure of the sample

Multi-slice calculation:

Calculation of the exit wave function for complex structures:

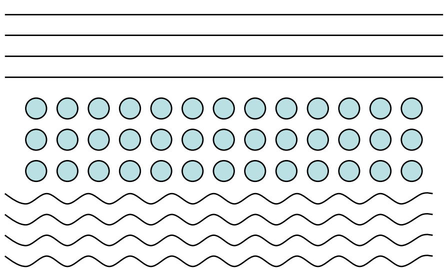

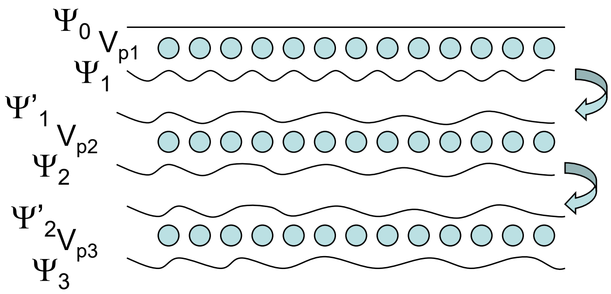

The sample is cut into thin slices

Transfer Function

- The optical system (lenses) can be described by a convolution with a transfer function T(x):
  Point spread function (PSF): describes how a point on the object side is transformed into the image.

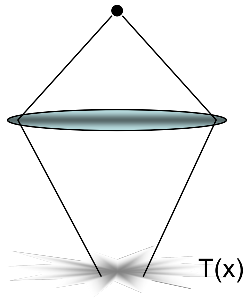

$$\Psi_i(\underline{x}) = \int_{-\infty}^{\infty} \Psi_o(\underline{u}) T(\underline{x} - \underline{u}) d\underline{u} = \Psi_o(\underline{x}) \otimes T(\underline{x})$$

- ***Transfer Function***:
  desscribe how an "objet" wave-function is transformed into an "image" wave-function

$$\Psi_i(\underline{h}) = \Psi_o(\underline{h}) T(\underline{h})$$

- **The image INTENSITY** observed on a screen (or a camera / negative plate etc.)

$$I_i(\underline{x}) = \Psi_i(\underline{x}) \Psi_i^*(\underline{x})$$

$$I_i(\underline{h}) = \Psi_i(\underline{h}) \otimes \Psi_i^*(-\underline{h}) = \int \Psi_i(\underline{h}') \Psi_i^*(\underline{h} - \underline{h}') d\underline{h}'$$

$$I_i(\underline{h}) = [\Psi_o(\underline{h}) T(\underline{h})] \otimes [\Psi_o^*(-\underline{h}) T^*(-\underline{h})]$$

Coherent Transfer Function (CTF) of magnetic lens

$$T(\vec{\mathbf{h}}) = \exp\left[2\pi i \chi(\vec{\mathbf{h}})\right]$$

$$\chi(\vec{\mathbf{h}}) = 0.25 C_s \lambda^3 h^4 + 0.5 \Delta z \lambda h^2$$

Spherical aberration defocus

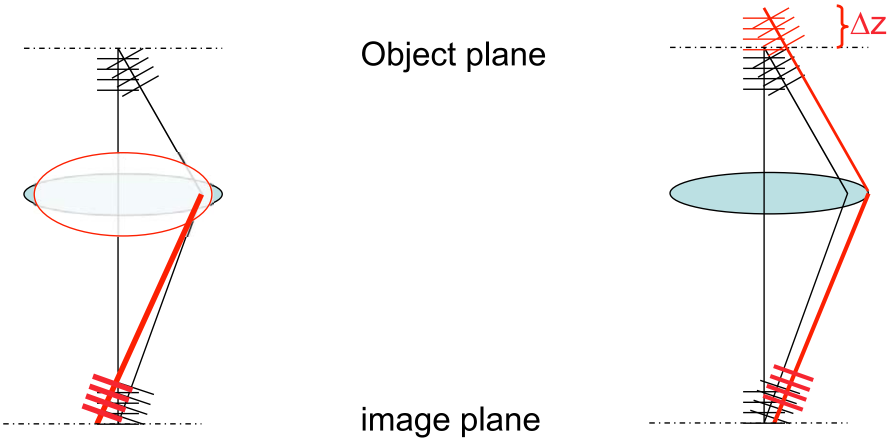

The « magic » of image contrast

Objet de Phase Faible (Weak Phase Object)

$$\Psi_o(\underline{x}) = exp[-i\sigma V_p(\underline{x};z)] \cong 1 - i\sigma V_p(\underline{x};z)$$

$$\Psi_o(\underline{h}) = \delta(\underline{h}) - i\sigma V_p(\underline{h})$$

$$\Psi_i(\underline{h}) = \Psi_o(\underline{h})T(\underline{h}) = \Psi_o(\underline{h})exp[2\pi i\chi(\underline{h})]$$

$$\Psi_i(\underline{h}) = [\delta(\underline{h}) - i\sigma V_p(\underline{h})][\cos 2\pi\chi(\underline{h}) + i\sin 2\pi\chi(\underline{h})]$$

Fourier Space

En choisissant $\sin[2\pi\chi(\mathbf{h})] = -1$ et $\cos[2\pi\chi(\mathbf{h})] = 0$ pour les réflexions **h** les plus intenses, $\Psi_i(\mathbf{h})$

Fonction d'onde image

$$\Psi_i(\underline{h}) = \delta(\underline{h}) - \sigma V_p(\underline{h})$$

L'intensité de l'image ($\Psi_i(\underline{\mathbf{x}})\ \Psi_i^*(\underline{\mathbf{x}})$) est alors donnée par :

Intensité de l'image de l'objet faible en contraste direct

$$I(\underline{x}) = (1 - \sigma V_p(\underline{x}))(1 + \sigma V_p(\underline{x})) = 1 - 2\sigma V_p(\underline{x}) + O(\sigma^2 V_p^2(\underline{x}))$$

but....

En choisissant $\sin[2\pi\chi(\underline{\mathbf{h}})] = 0$ et $\cos[2\pi\chi(\underline{\mathbf{h}})] = 1$, l'intensité de l'image ($\Psi_i(\underline{\mathbf{x}})\ \Psi_i^*(\underline{\mathbf{x}})$) est puisque $\Psi_i(\underline{\mathbf{h}})$ égale:

Fonction d'onde image

$$\Psi_i(\underline{h}) = [\delta(\underline{h}) - i\sigma V_p(\underline{h})]$$

Intensité de l'image de l'objet faible en contrast inverse

$$I(\underline{x}) = (1 - i\sigma V_p(\underline{x}))(1 + i\sigma V_p(\underline{x})) = 1 + \sigma^2 V_p^2(\underline{x})$$

L'intensité est reliée linéairement au carré du potentiel projeté: ***l'interprétation en terme de colonnes atomiques et de canaux n'est plus aussi directe***.

For a direct and simple interpretation of the image contrast:
the imaginary part (sin) of the transfer function exp[2piχ(h)] should be ~1

The only free parameter in the microscope is: the defocus Δz

CTF

- CTF: contrast transfer function
  (« useful » = V_p)

$$CTF(k) = -\sin\left[\frac{\pi}{2} C_s \lambda^3 k^4 + \pi \Delta z \lambda k^2\right]$$

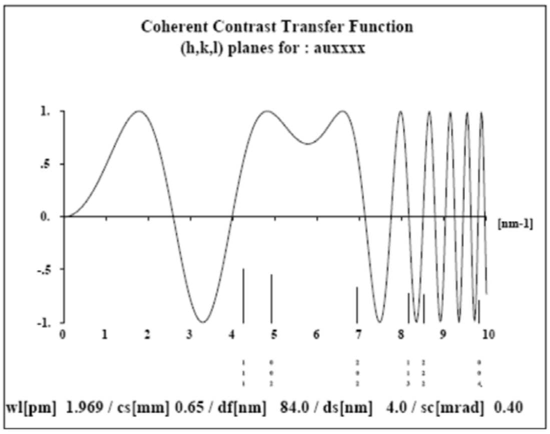

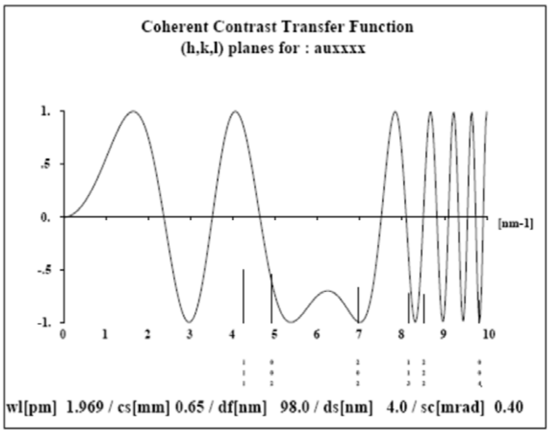

Scherzer defocus

With $\Delta z_{scherzer}$

$$\Delta z = -\sqrt{4/3\, C_s \lambda}$$

The CTF has a wide pass band

$$D_{scherzer} = 0.66 \lambda^{3/4} C_s^{1/4}$$

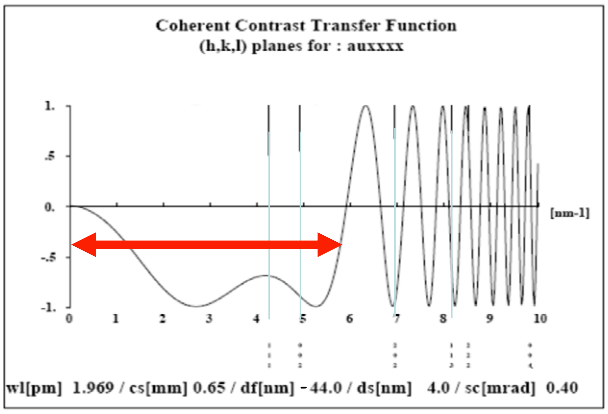

The first zero crossing of the CTF defines the « point-to-point » resolution of an electron microscope
The atom columns appear as dark areas on a bright background

$$I(\underline{x}) = (1 - \sigma V_p(\underline{x}))(1 + \sigma V_p(\underline{x})) = 1 - 2\sigma V_p(\underline{x}) + O(\sigma^2 V_p^2(\underline{x}))$$

CTF & spatial and temporal coherence « envelopes »

$$T(\vec{\mathbf{h}}) = a(\vec{\mathbf{h}})\exp\left[2\pi i\chi(\vec{\mathbf{h}})\right]E_s(\vec{\mathbf{h}})E_t(\vec{\mathbf{h}})$$

CM300UT FEG
Field emission
C_s: 0.7mm
Δz= 44nm

Résolution (point to point): 1.7Å
Information limite : ~1.2Å

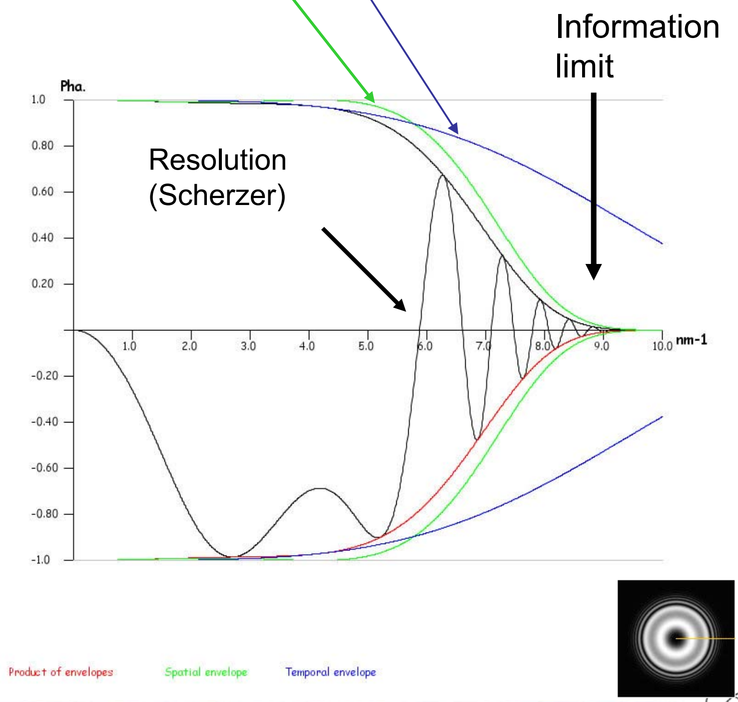

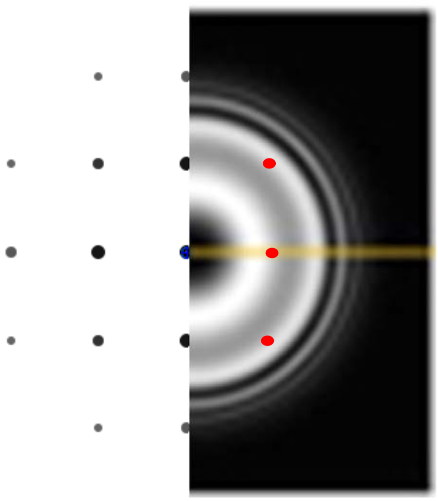

A good microscope

CM300UT FEG
Emmission à éffet de champs
C_s: 0.7mm
Δz= 44nm

Résolution (point à point): 1.7Å
Limite d'information: ~1.2Å

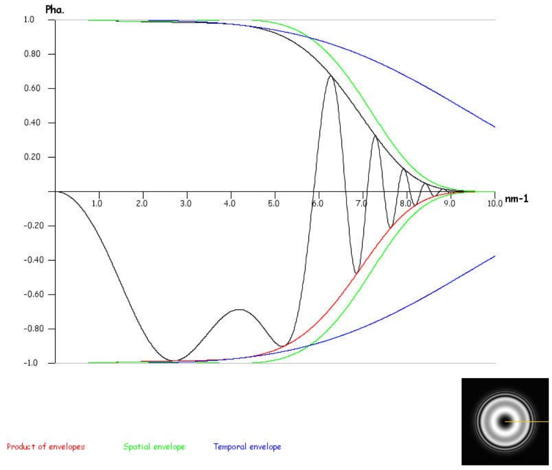

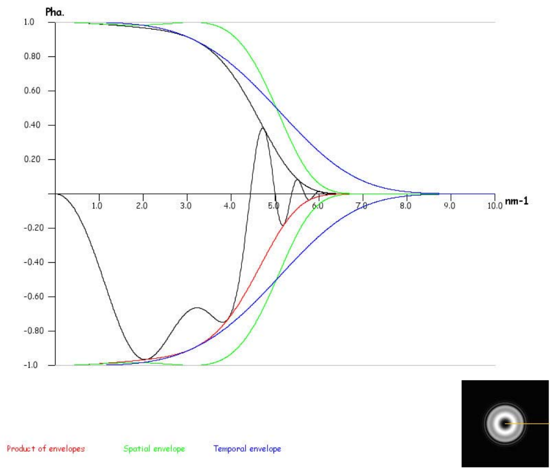

CM30ST LaB6
Emmission thermionique
C_s: 2mm
Δz= 76nm

Résolution (point à point): 2.1Å
Limite d'information: ~1.9Å

Super microscopes…..

Cs=0.2mm

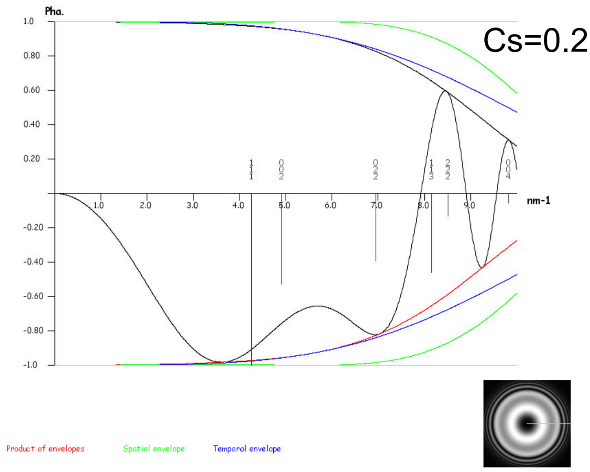

Cs=0.01mm

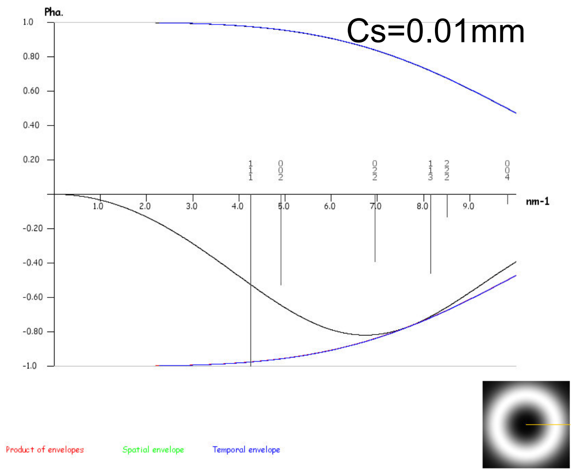

Dilemma: Cs=0mm: no more contrast….

Pass bands

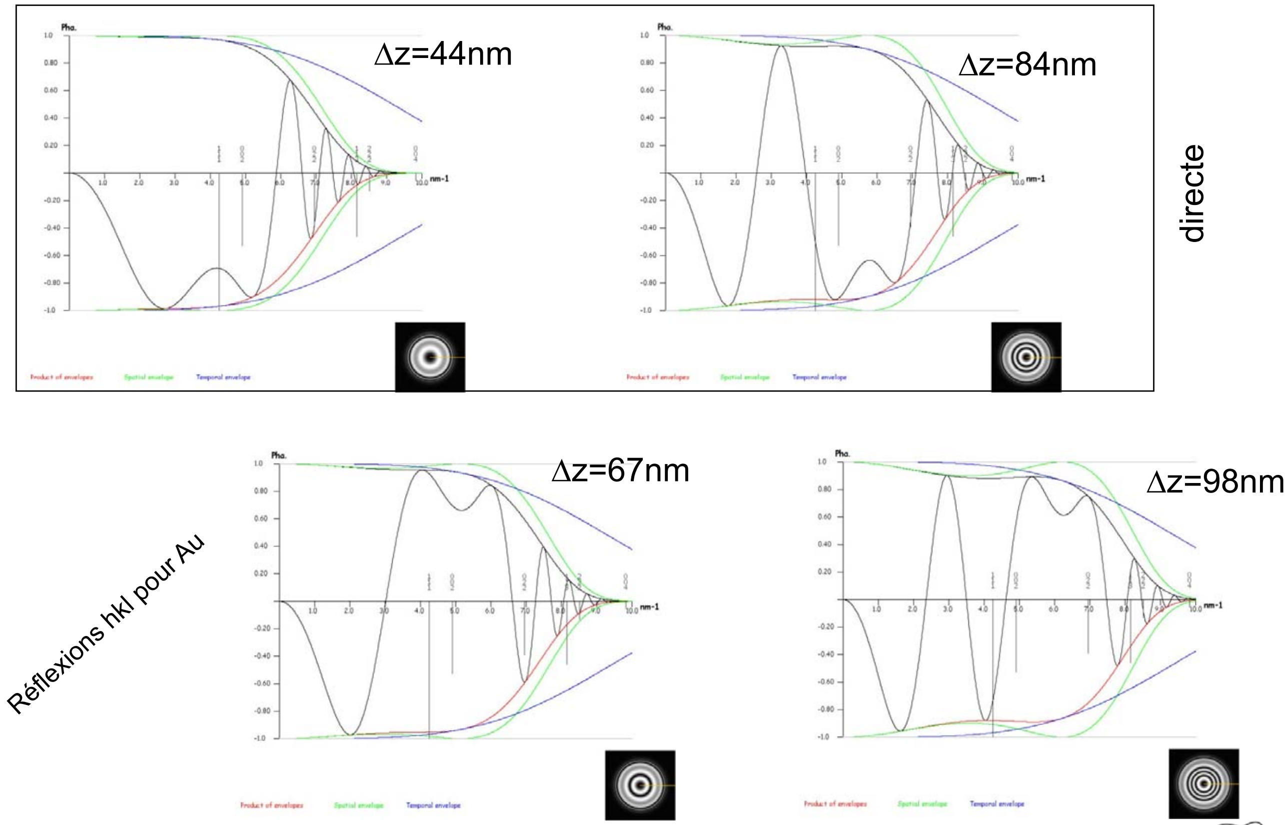

Defocus

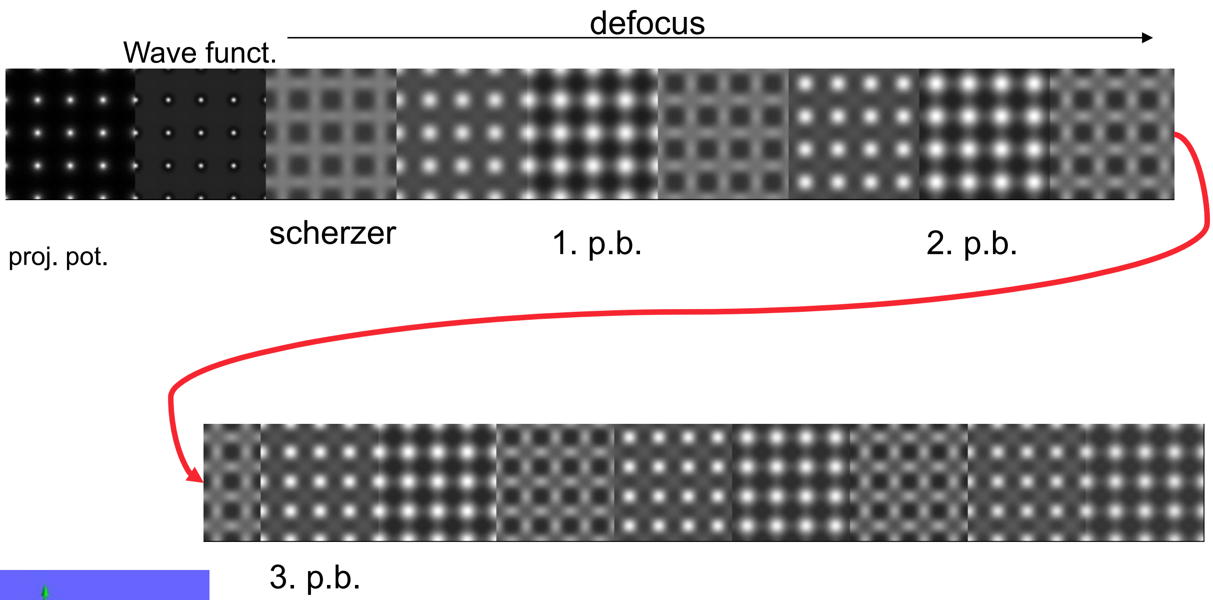

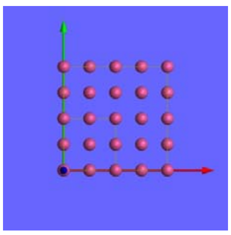

Au [100], thickness 20nm

HRTEM image formation

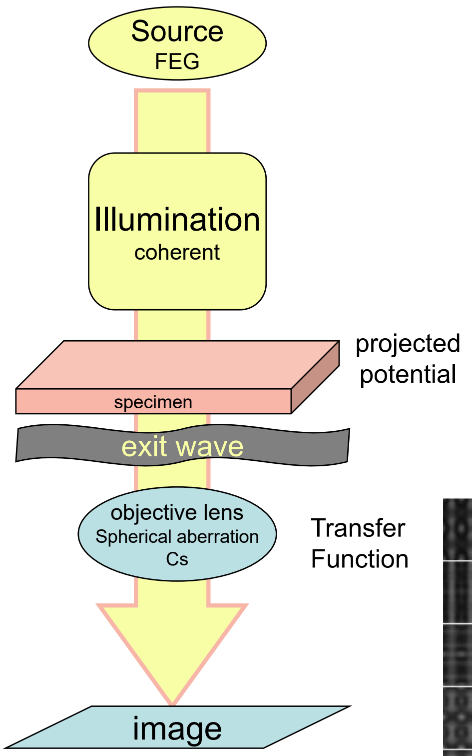

image of "projected potential"

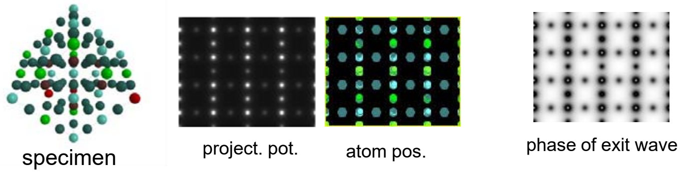

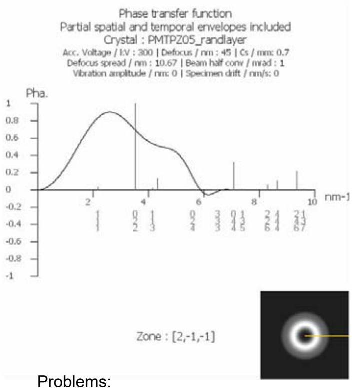

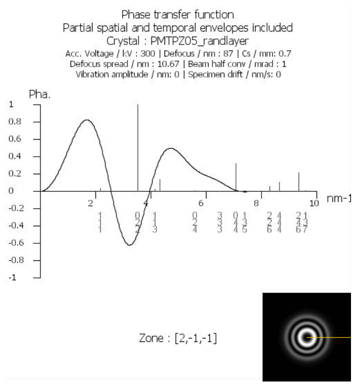

Problems:
defocusing for contrast: delocalization of information, information limit not used

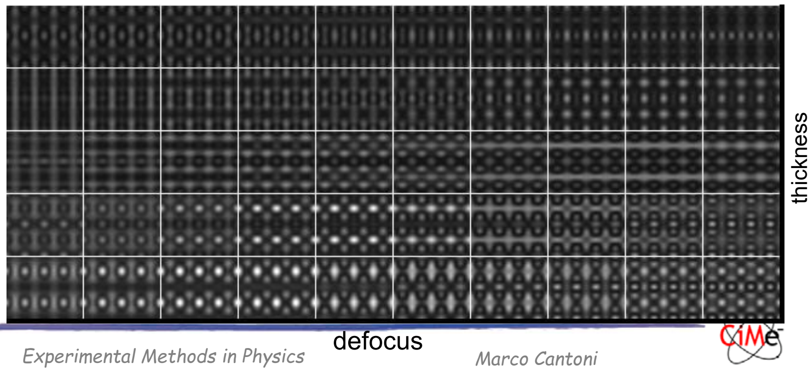

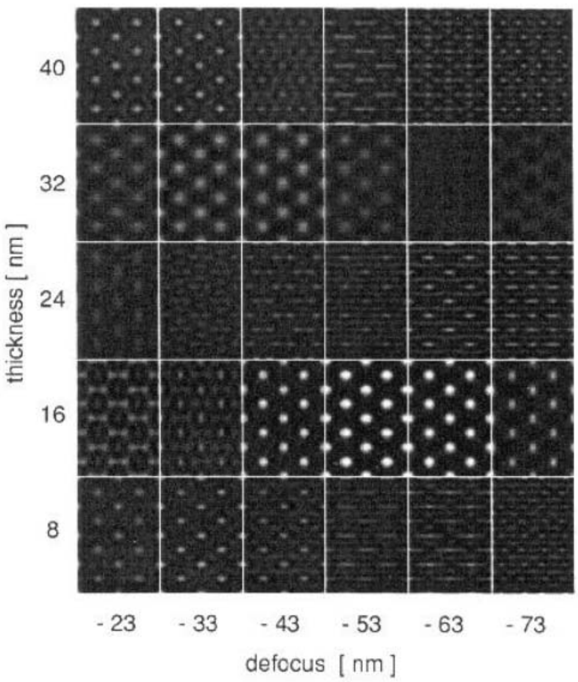

Thickness-defocus map in Fe3Al intermetallics
M. Karlik Materials structure, 8 (2001),3

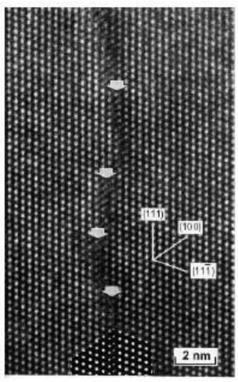

Experiment

What do you notice ?

Can you figure out the underlying explanation?

“delocalisation”

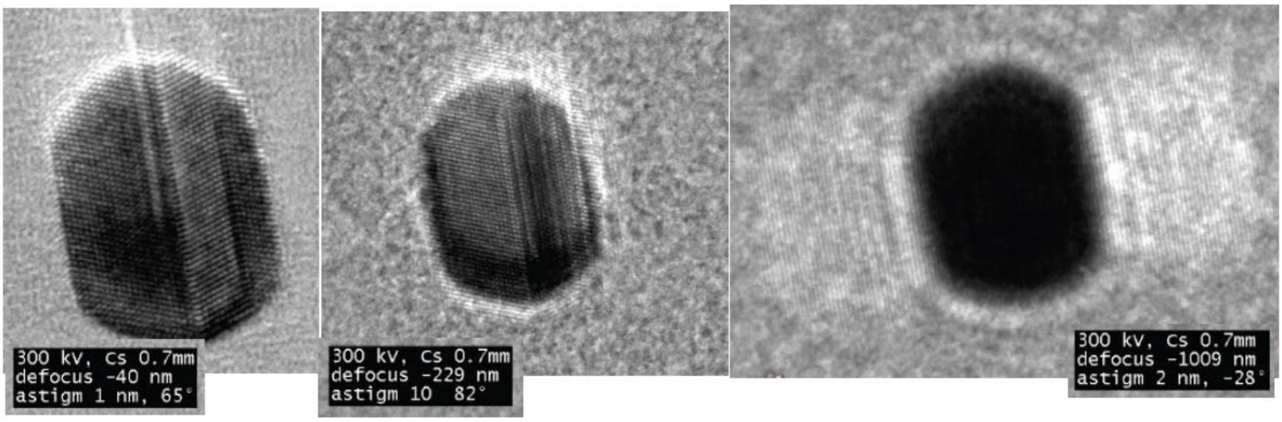

Au nanoparticle on amorphous carbon.Various defocalisation

HRTEM image formation

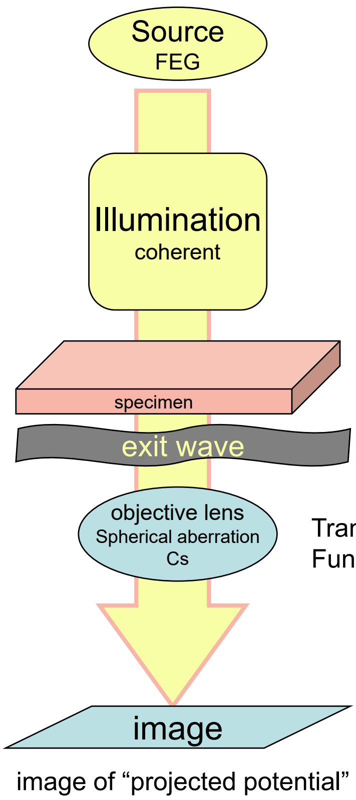

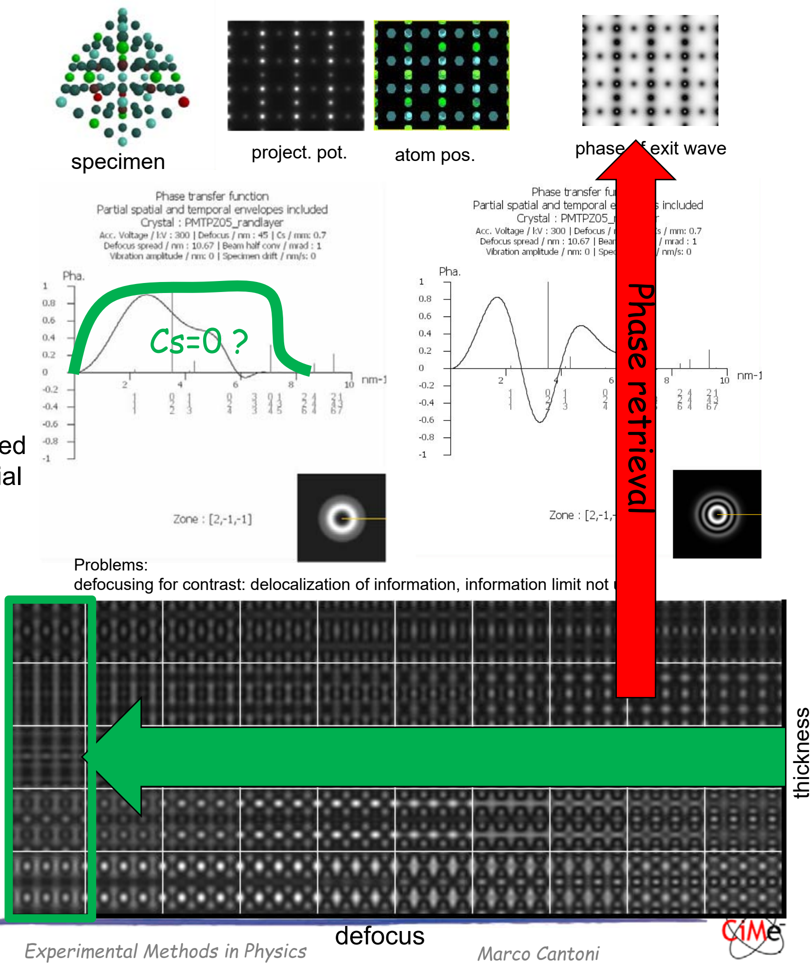

Exit wave function reconstruction

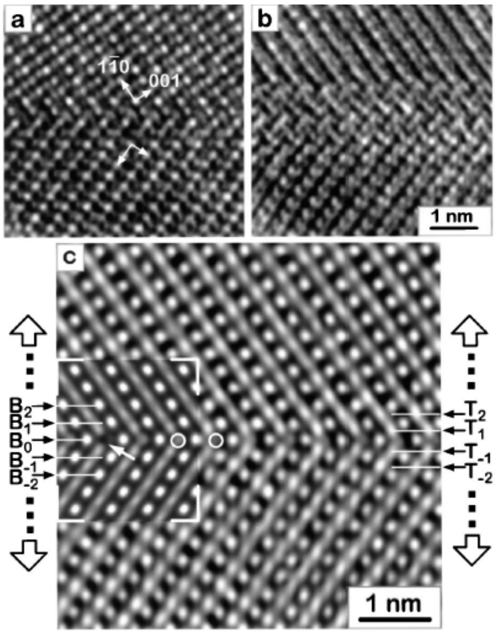

reconstructed phase of {111} twin boundary in perovskite BaTiO3

<110> zone axis. Phase of EPW reconstructed from series of 20 images with different defocus values.
The inset is a simulation for a specimen thickness of 2.8 nm. Circles denote oxygen columns located in the boundary plane. {111} Ti planes are labeled with "*T*" and {111} Ba-O planes with "*B*".

C. L. Jia and A. Thust
PHYSICAL REVIEW LETTERS 82, 25

Iterative Wave Form Reconstruction: IWFR
FEI: TrueImage

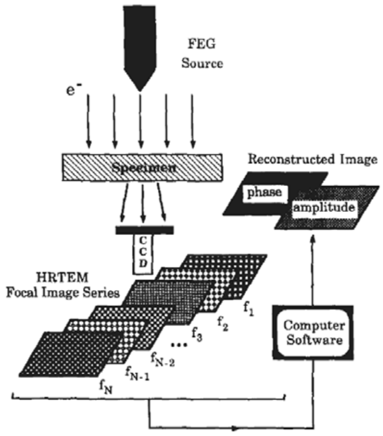

A. Thust, M.H.F. Overwijk, W.M.J. Coene, M. Lentzen
Ultramicroscopy 64 (1996) 249-264

L.J. Allen, W. McBride, N.L. O'Leary, M.P. Oxley
Ultramicroscopy 100 (2004) 91–104

corrector s

- Astigmatisme
  - Optique: correction avec une lentille cylindrique
  - EM: correction avec un stigmateur: quadrupôle
    - Image d'un point = ligne
    - Deux quadrupôles montés à 45° permettent d'ajuster la force et la direction de la correction
- Abbération sphérique
  - Optique: utilisation de lentilles avec des surfaces non-sphériques
  - EM: combinaison de quadrupôles et d'octopôles

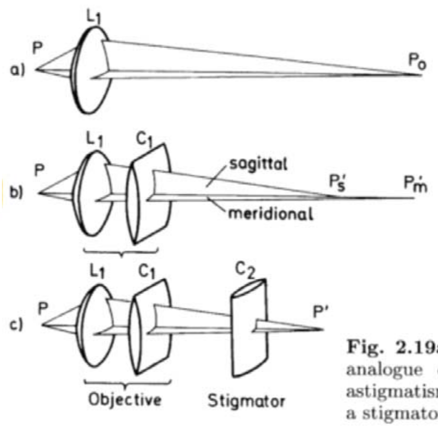

Fig. 2.19a–c. Light-optical analogue of the action of astigmatism (L1 + C1) and a stigmator C2 [2.30]

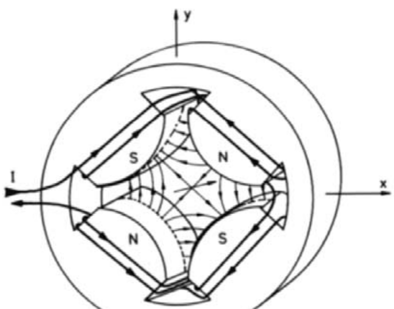

Fig. 2.12. Construction of a quadrupole lens

Aberration Correction

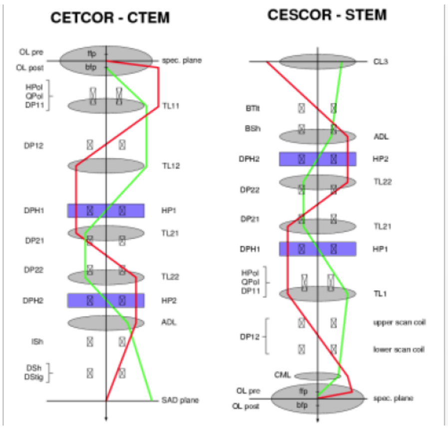

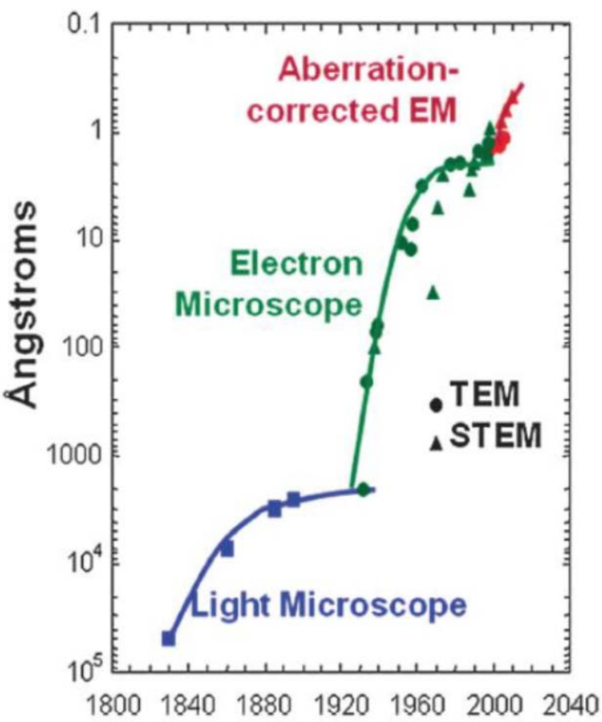

the aberration-corrected transmission electron microscope

(Rose, 1990; Haider et al., 1998)

Maximilian Haider, Stephan Uhlemann,
Eugen Schwan, Harald Rose, Bernd Kabius, Knut Urban
NATURE, VOL 392, 1998

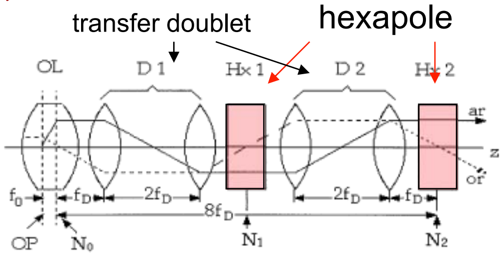

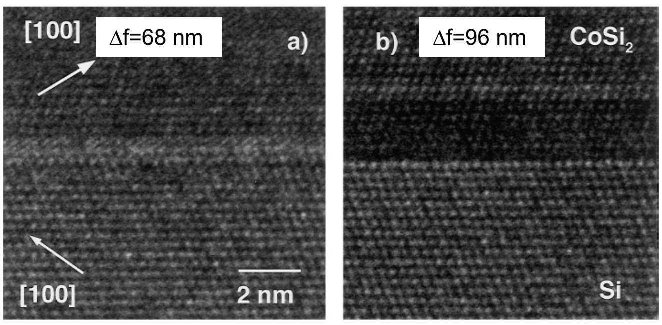

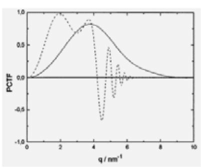

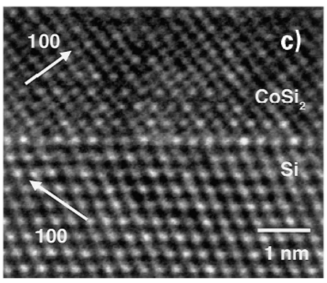

- Cs-corrector

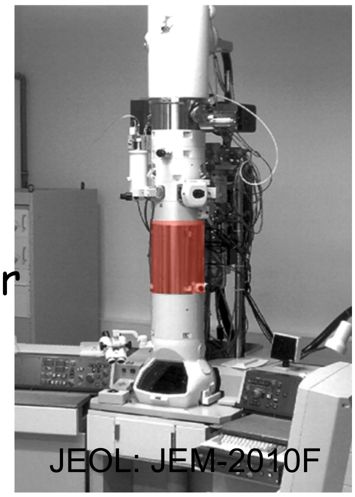

Super microscopes…..

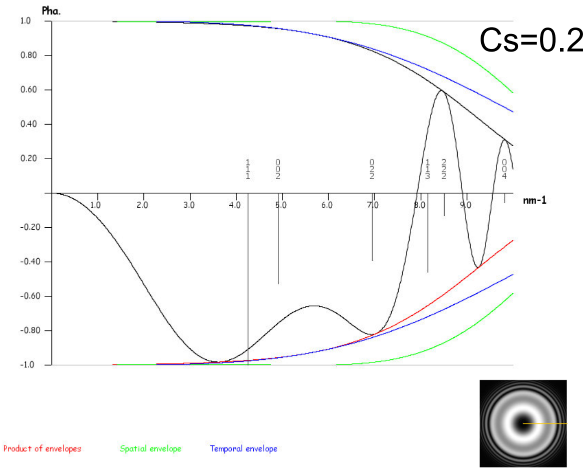

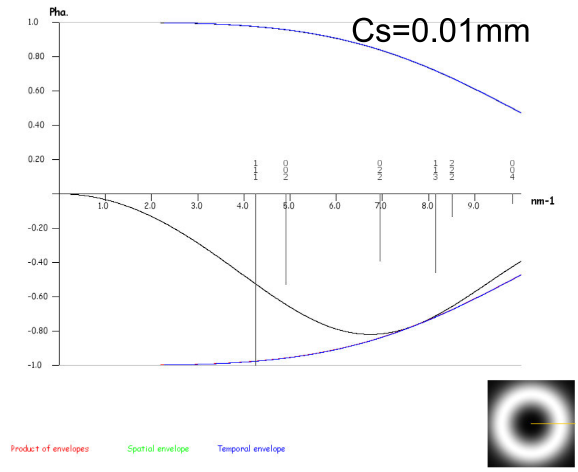

Dilemma: Cs=0mm: no more contrast for low space frequencies….

Cs correctors 2008: FEI Titan

Breaking the spherical and chromatic aberration barrier in transmission electron microscopy

B. Freitag, S. Kujawa, P.M. Mul, J. Ringnalda*, P.C. Tiemeijer

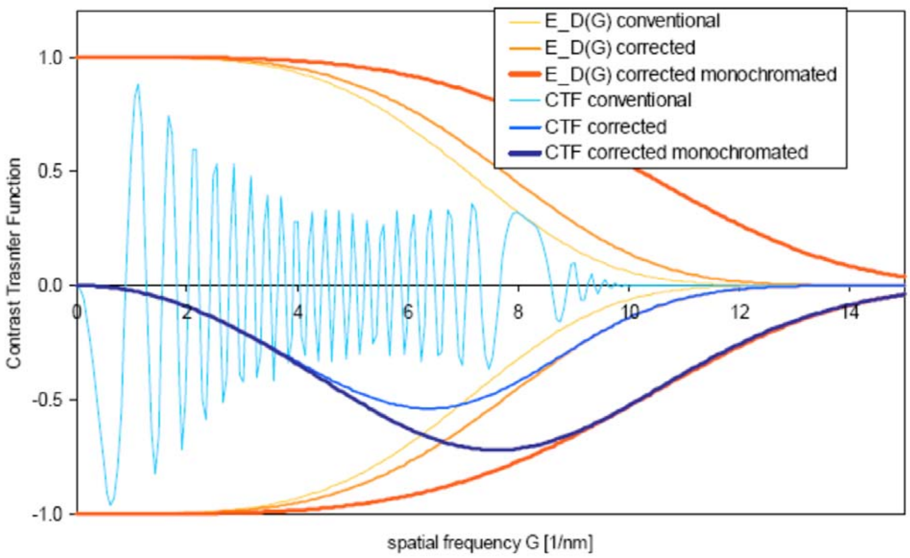

Sharp interfaces

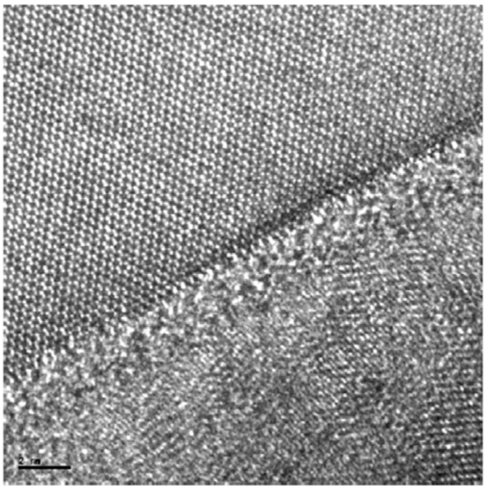

Fig. 3. TEM image of a cross section of a MOSFET transistor showing the amorphous gate oxide layer between crystalline silicon and polycrystalline silicon, recorded with monochromator on and Cs corrector on. The image was taken with 0.1 nA beam current on the CCD, 1 s exposure time, and 2 mrad half convergence angle.

No delocalisation at interfaces anymore

Cs corrector off

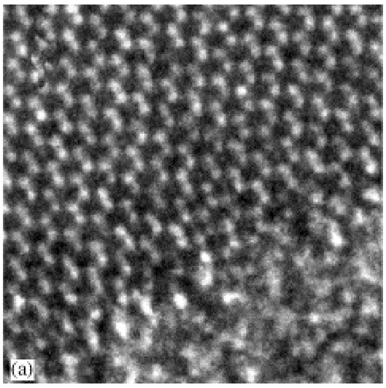

Cs corrector on

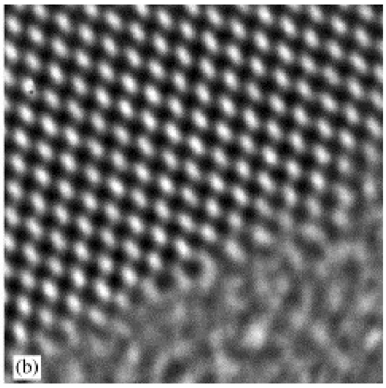

Gold crystal

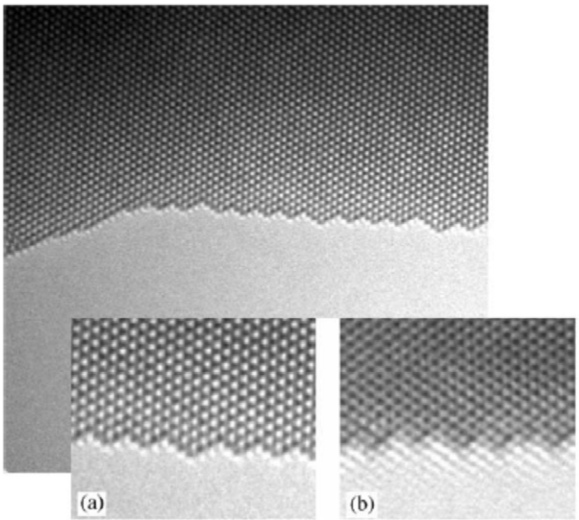

Fig. 5. Images of gold crystal recorded with monochromator on and Cs corrector on, with insets illustrating the difference between Cs corrector on and Cs corrector off: (a) The edge is clearly imaged, without fresnel fringes or delocalization effects. (b) The image without Cs correction, illustrating the difficulty of directly interpreting an image from a conventional field emission gun system.

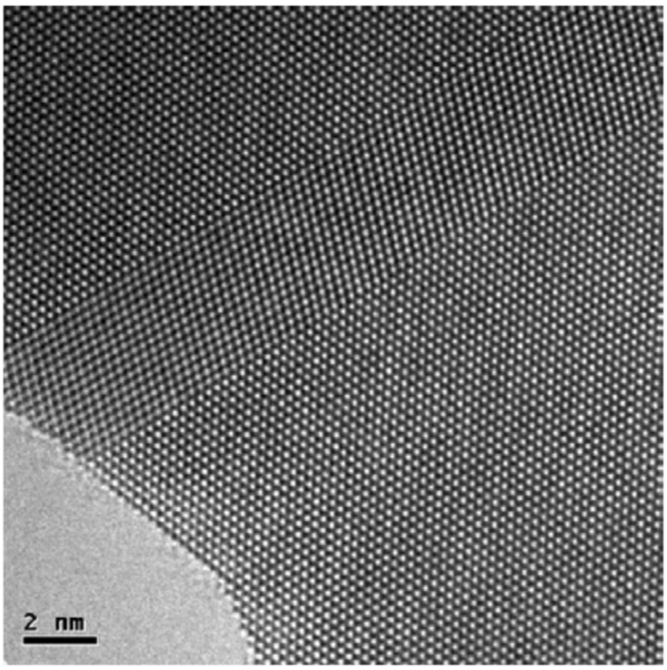

5. SCANNING Transmission Electron Microscopy

STEM

High-Resolution STEM

HAADF

b) CTEM/SEM principles

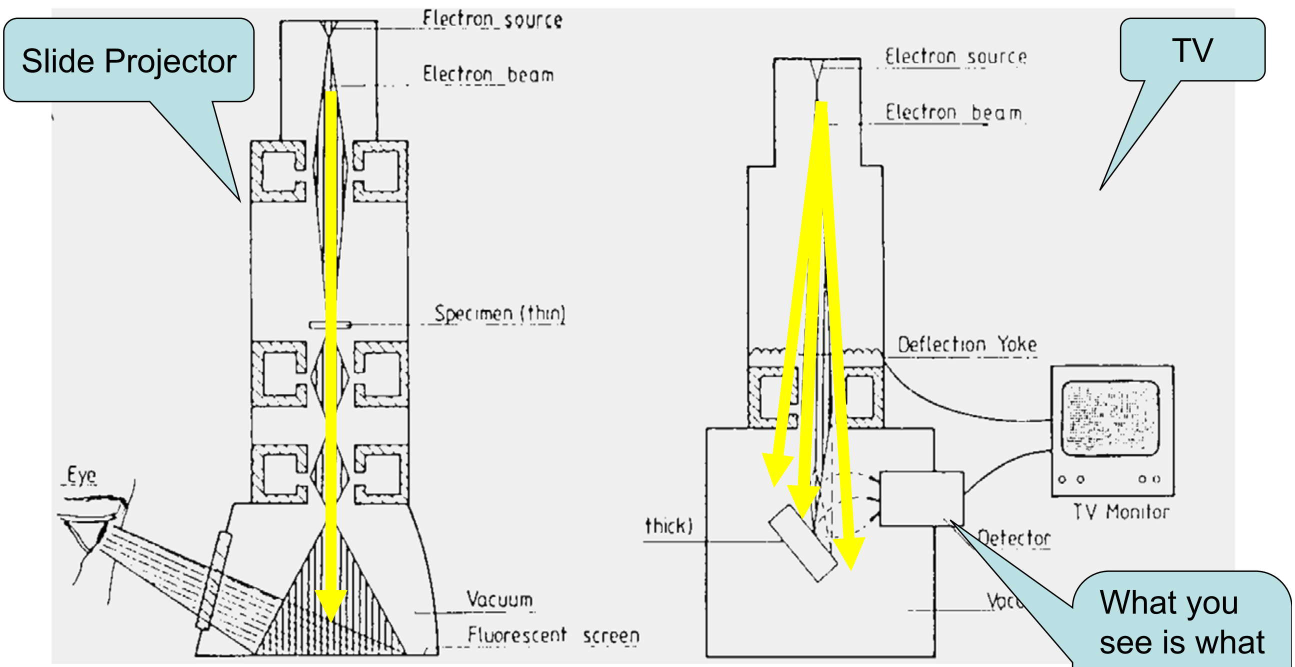

Conventional Transmission Electron Microscope

Scanning Electron Microscope

TEM-SEM
interaction of electrons with the sample

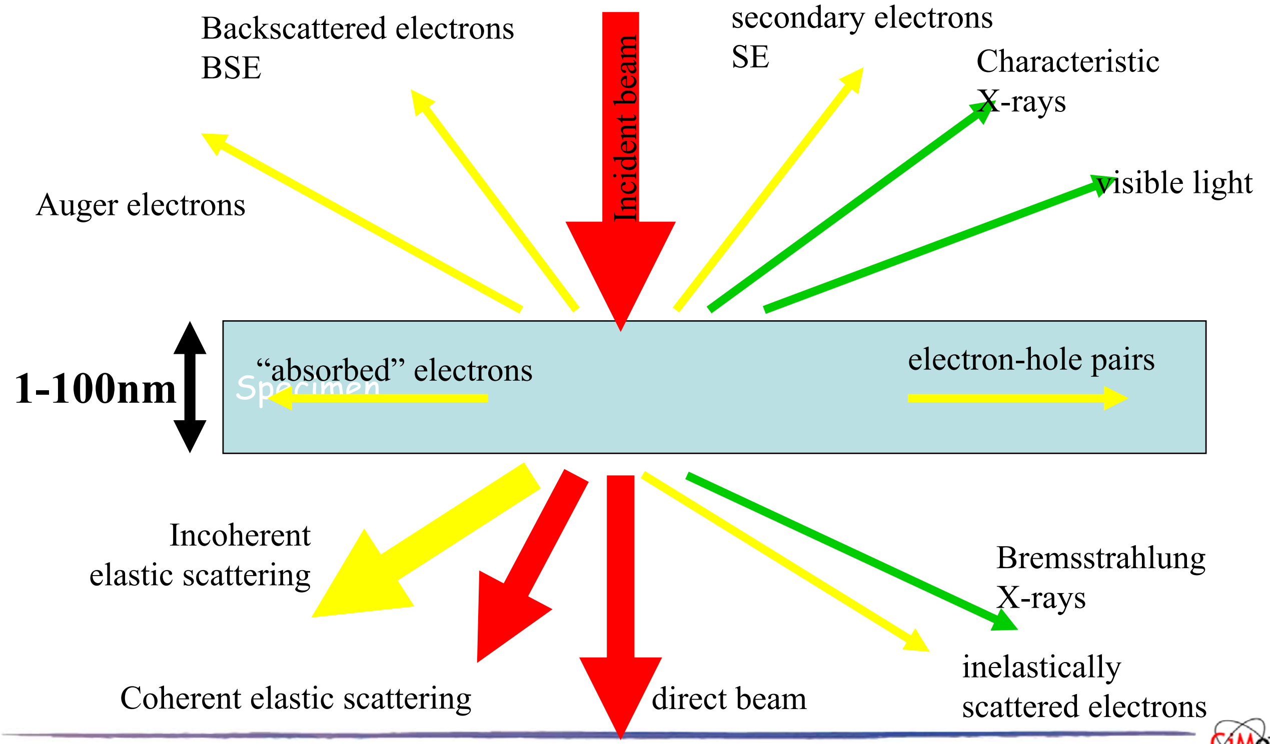

Reciprocity

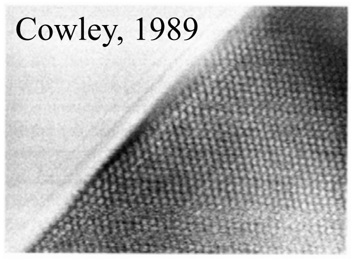

Figure 3. Bright-field STEM image of a small MgO crystal in [1 1 0] orientation [95].

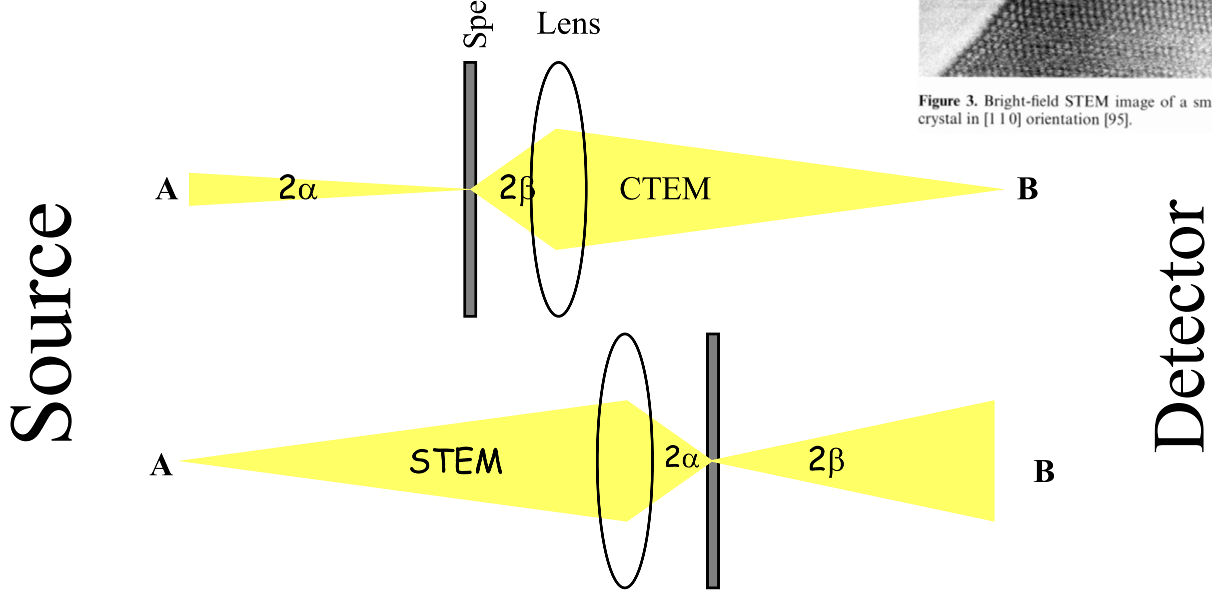

Cowley (1969): for the same lenses, apertures and system dimension the image contrast must be the same for CTEM and STEM

$2\alpha_{STEM} = 2\beta_{CTEM}$

$2\beta_{STEM} = 2\ \alpha_{CTEM}$

Microscope is operated in diffraction mode
Diffraction pattern = stationary pattern
BF/DF detectors

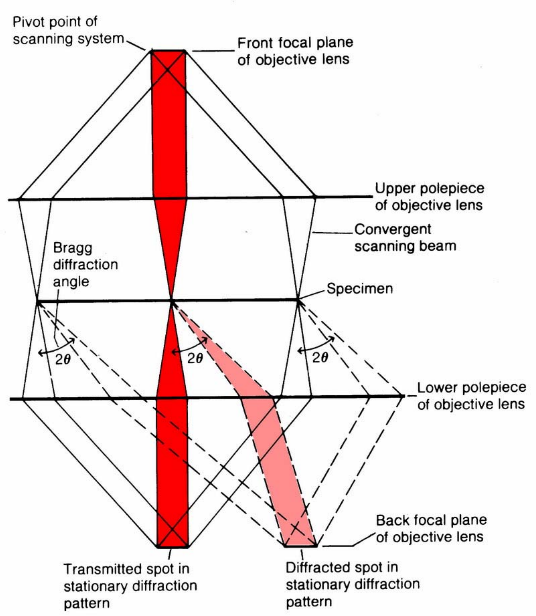

Figure 1.7. Stationary diffraction pattern formation in STEM.

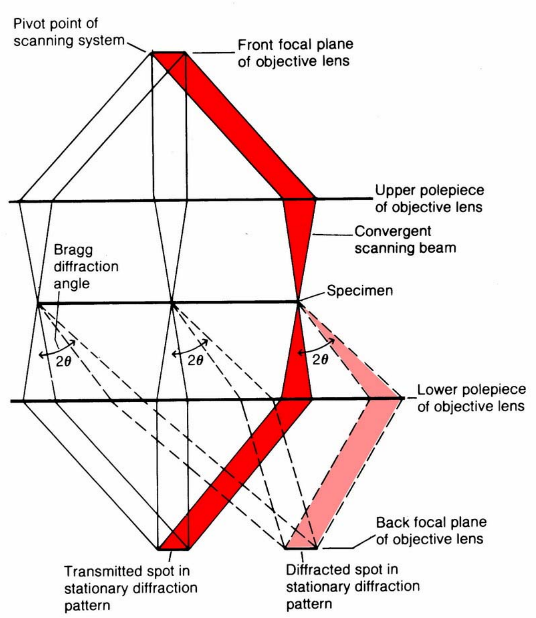

Figure 1.7. Stationary diffraction pattern formation in STEM.

Au particles on a C film

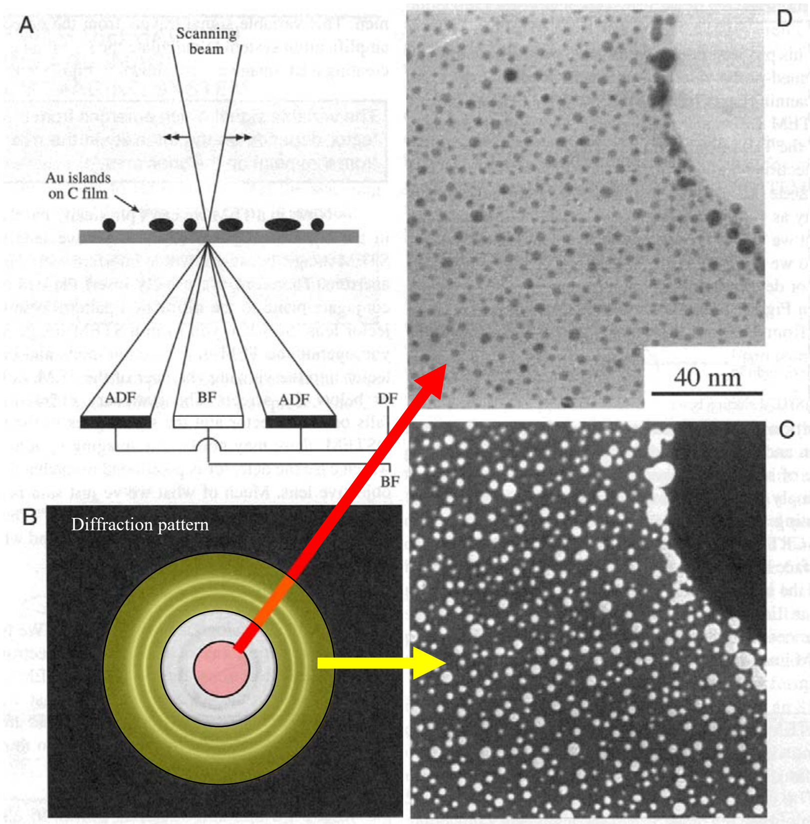

Microscope is in diffraction mode
Detectors placed relative to diffraction pattern

STEM BF:

Detection of transmitted electrons:

contrast similar to

CTEM BF image (objective aperture selects only transmitted electrons)

STEM ADF:

Detection of diffracted electrons on the annular DF detector:

(integration of multiple CTEM DF images)

Bright field/ AnnularDark field detector

influence of camera length and convergence angle

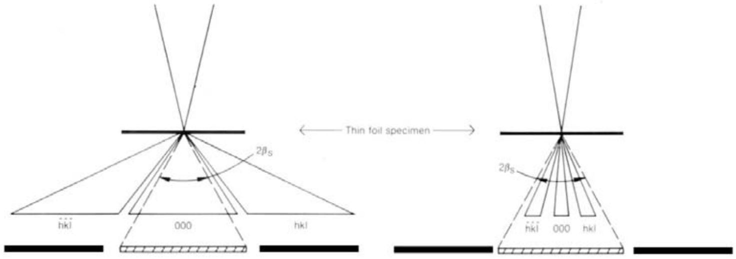

Big camera length small camera length

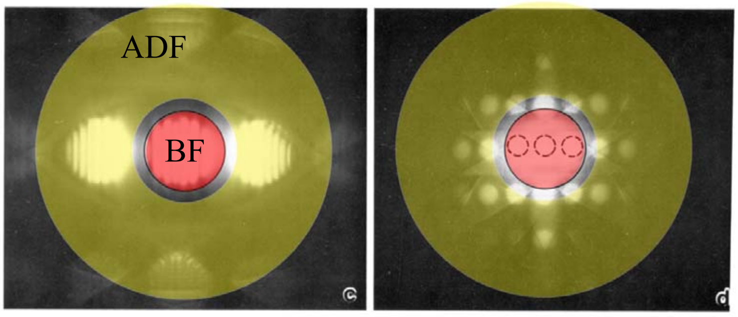

The selected camera-length (magnification of the diffraction pattern) determines what the detectors "sees"

Bright field TEM <->STEM

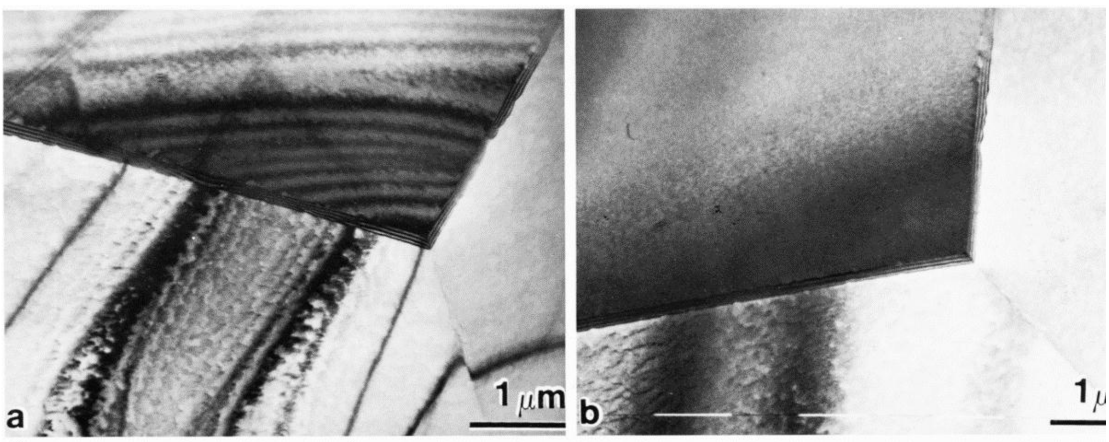

Figure 3.3a. Triple point in pure Al (TEM BF).

Figure 3.3b. Triple point in pure Al (STEM BF, $2\beta_S \sim 6 \times 10^{-3}$ rads, probe size $\sim$ 5 nm).

ADF STEM

Single atoms (or small groups of atoms) of Pt on crystalline Al_2O_3

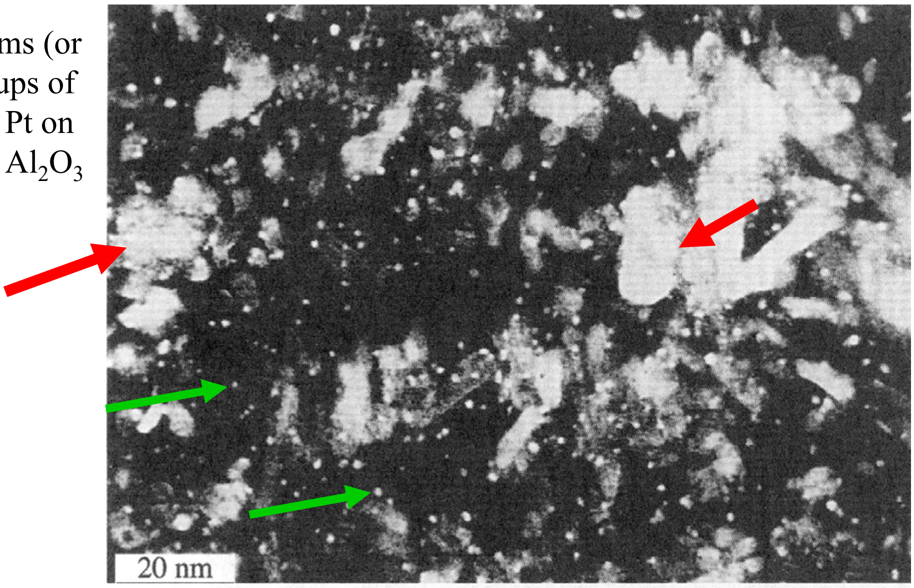

- The ADF image provides a signal which depends strongly on the bragg scattering (Al_2O_3). ***DIFFRACTION CONTRAST***
- **Single atoms scatter electrons incoherently to higher angles ~ *"z-contrast"***

c) High Angle Annular Dark Field

z-contrast
(atomic resolution)

- Ultramicroscopy 30 (1989) 58-69
- North-Holland, Amsterdam
- **Z-CONTRAST STEM FOR MATERIALS SCIENCE**
- S.J. PENNYCOOK

- Ultramicroscopy 37 (1991) 14-38;
- North-Holland
- **High-resolution Z-contrast imaging of crystals**
- S.J. Pennycook and D.E. Jesson

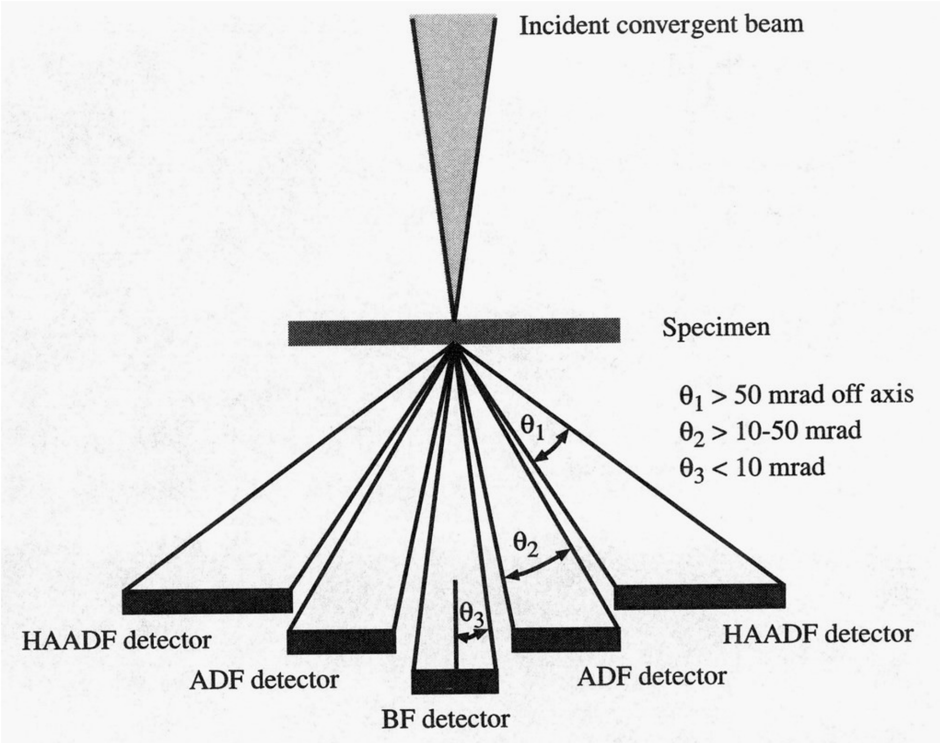

High Angle Annular Dark field detector

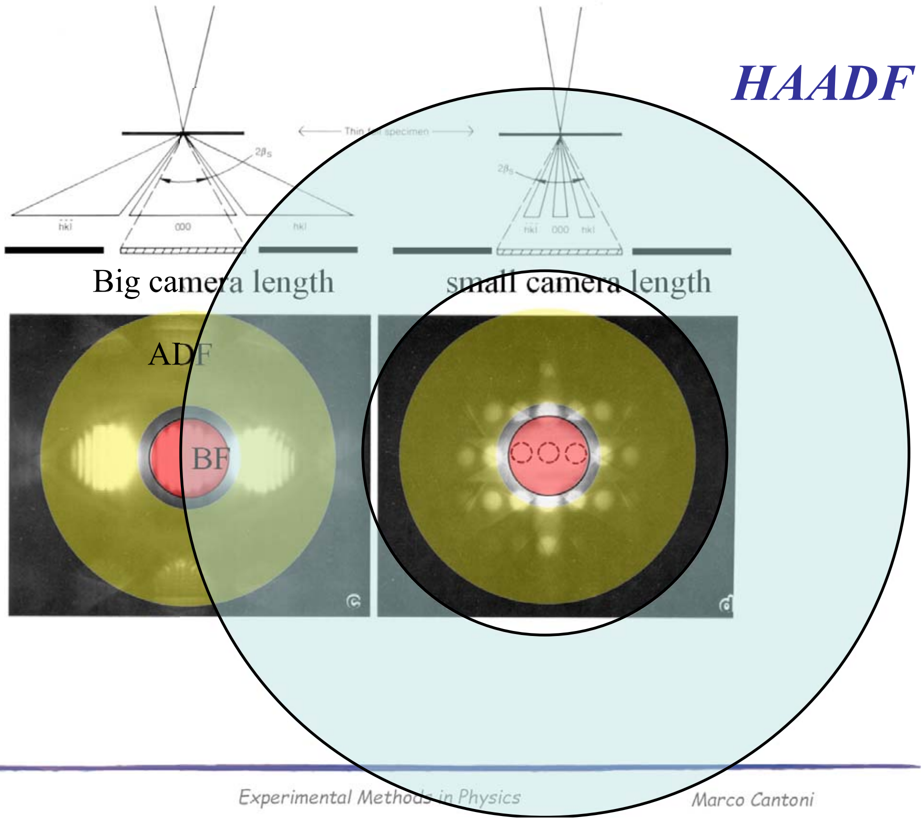

High angle incoherent scattering

- The annular DF detector is placed beyond the **bragg-scattered** electrons…
- Small camera length and large diameter of the detectors inner diameter

The image is formed by high angle incoherently scattered electrons -> Rutherford scattering at the nucleus of the atoms

$\sigma \sim z^2$

Z-Contrast

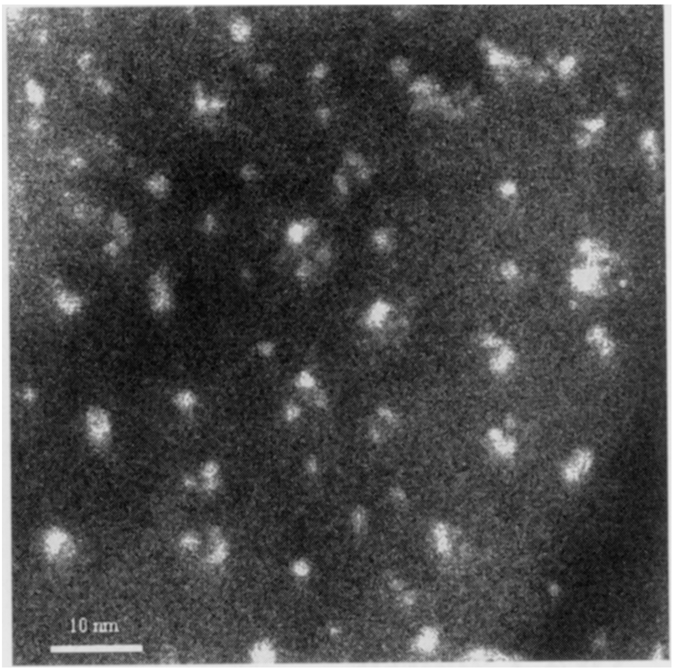

Si nano-crystals in SiO_2 formed by implantation

HAADF <-> HRTEM

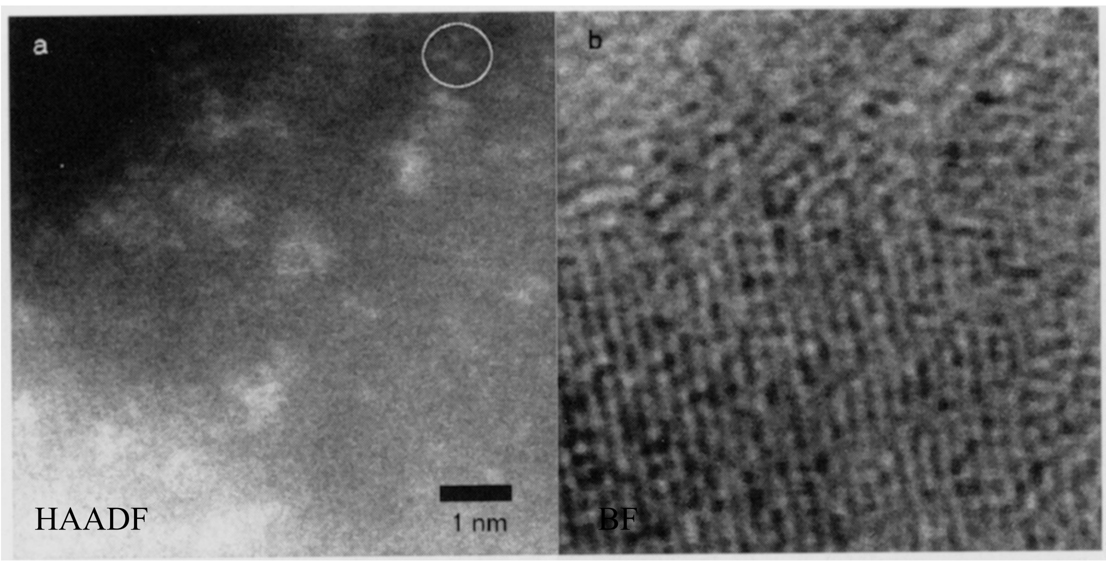

- Pt catalyst on Al_2O_3
- Pt particles become visible in the HAADF image

HRTEM <-> STEM HAADF

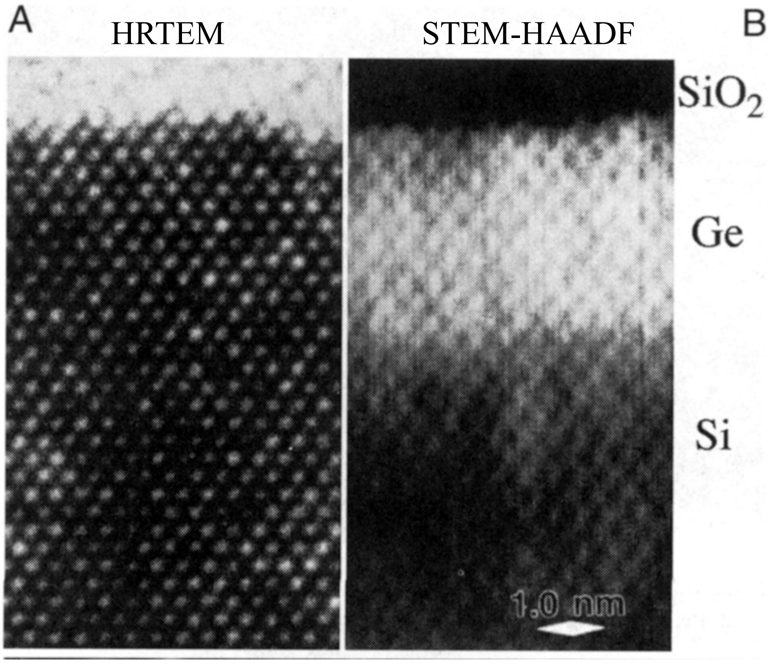

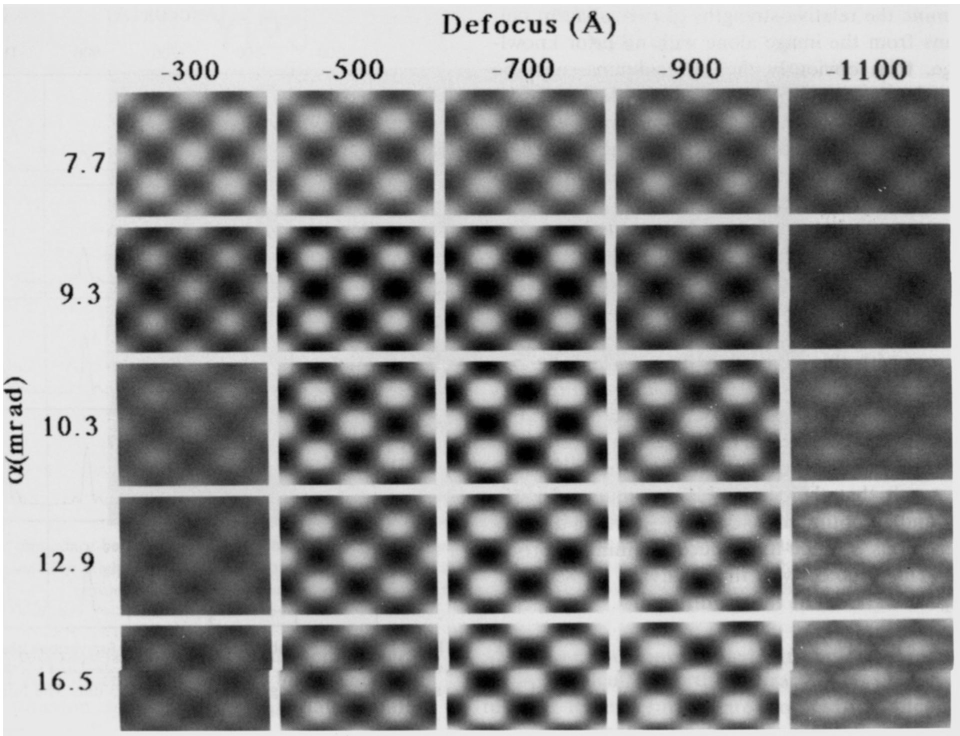

Fig. 12. Simulated images of Si⟨110⟩ corresponding to the probes shown in fig. 11.

No contrast reversal as in CTEM HRTEM images !!!!
no repeated contrast patterns at different defocus settings

HAADF-STEM study of β'-type precipitates in an over-aged Al–Mg–Si–Ag alloy

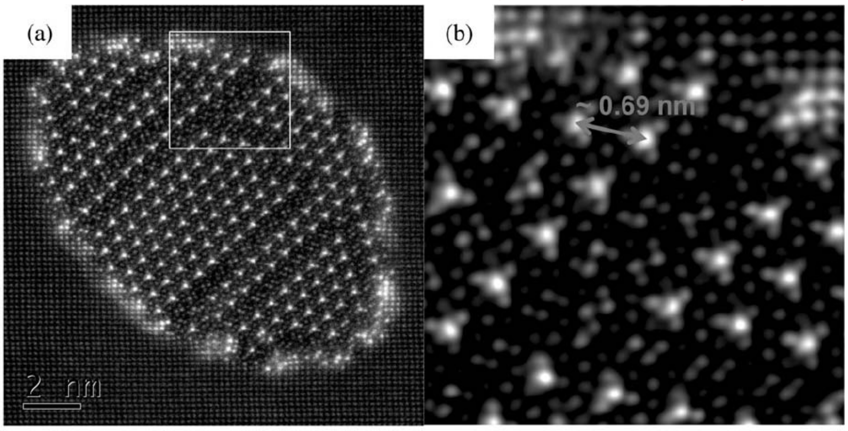

Figure 2. (a) Unprocessed high-angle annular dark field scanning transmission electron microscopy image of a typical precipitate rod-section, consisting of ordered β'_{Ag} domains separated by anti-phase resembling boundaries. The white box delimits an area shown enlarged in (b). (b) Noise in the enlarged image was filtered by applying a circular band pass mask that removed all distances shorter than 0.12 nm. Periodicity in the hexagonal plane of the β'_{Ag} phase is indicated. (c) Atomic overlay on the delimited area that was further enlarged. The unit cells of β'_{Ag} and $U2_{Ag}$ are overlaid using dark and white thick lines respectively; the Si columns belonging to a β'_{Ag} domain are connected by full thin white lines. Across the boundaries they are connected by thin dashed white lines; Mg atomic columns delimiting the domains while being part of the boundaries are connected by thick triple white lines. The Al atomic columns corresponding to Ag-free U2 are shown as circles with dotted lines, and the Al atomic columns in the model of β'_{Ag} from Table 1 are shown as circles with dashed lines.

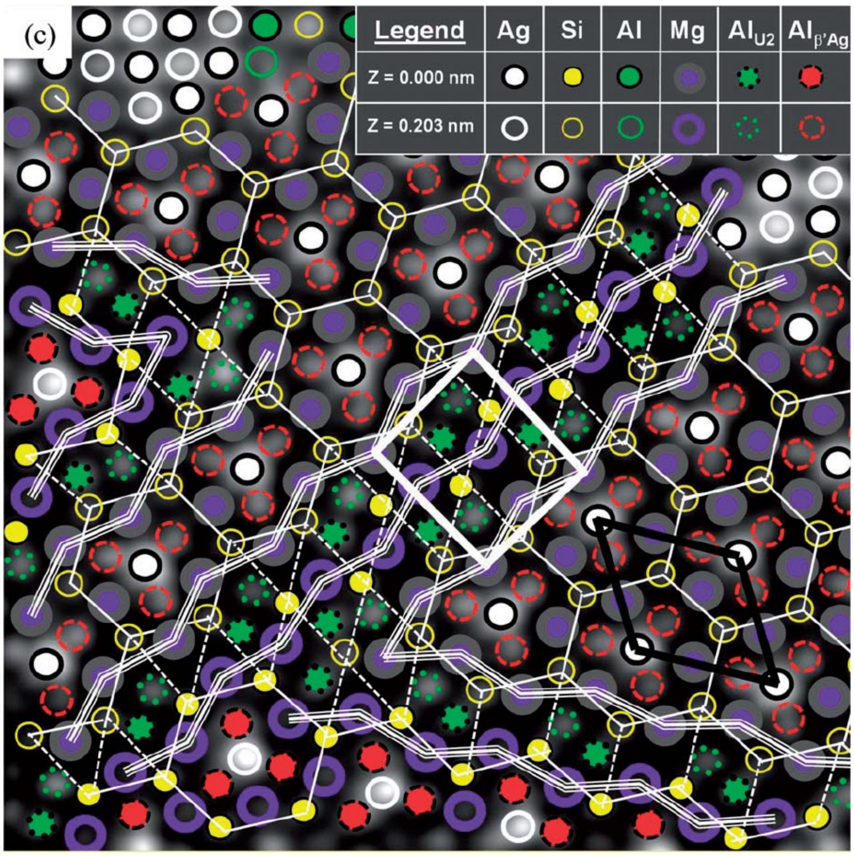

October 2014: Titan THEMIS @CIME

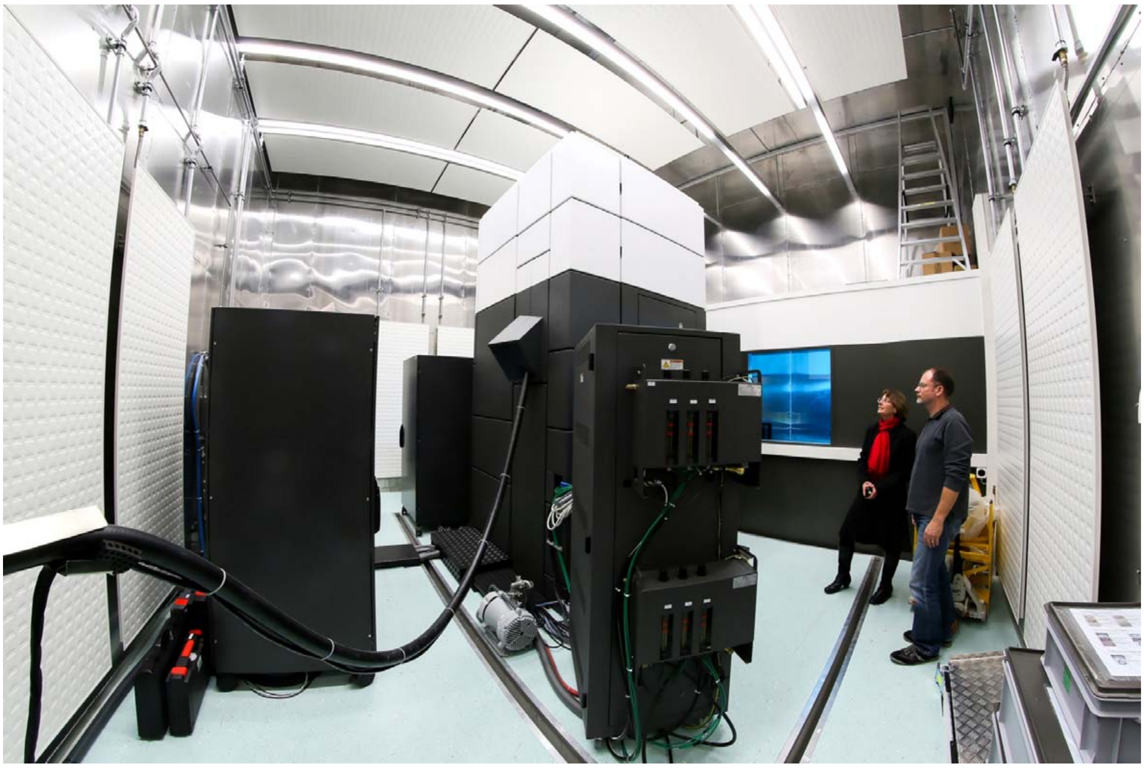

Chemical analysis on atom columns

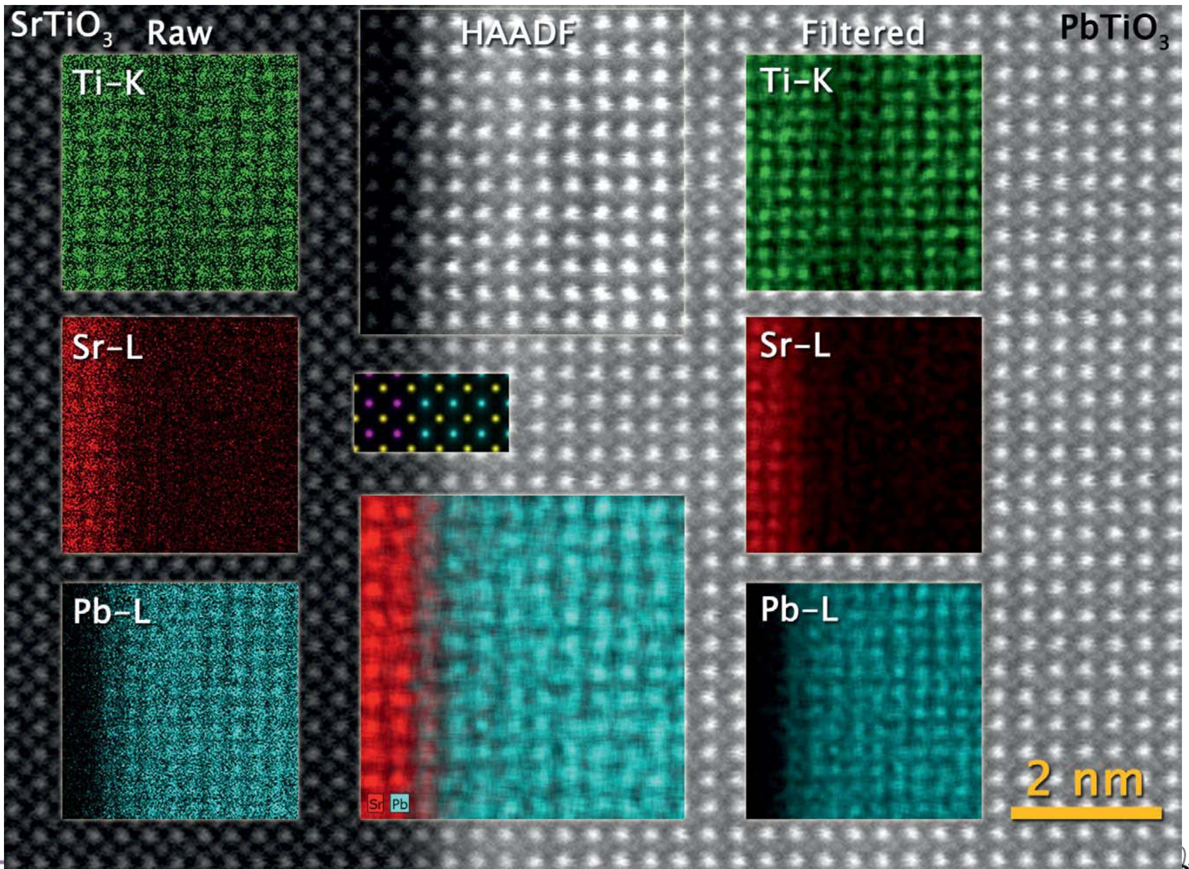

EPFL Titan THEMIS 7.11.2014